

**LC3-associated Phagocytosis induced by the β_2 integrin Mac-1
enhances Immunity to Infection with *Listeria monocytogenes***

Inaugural-Dissertation

zur

Erlangung des Doktorgrades

der Mathematisch-Naturwissenschaftlichen Fakultät

der Universität zu Köln

vorgelegt von

Alexander Gluschko

aus Kiewka

Köln 2018

Berichterstatter: Prof. Dr. Thorsten Hoppe

Prof. Dr. Martin Krönke

Tag der letzten mündlichen Prüfung: 20.06.2018

Table of Contents

List of Abbreviations	4
1 Introduction	7
1.1 Macrophages	7
1.1.1 Mac-1	8
1.1.2 Acid sphingomyelinase	9
1.1.3 NADPH oxidase 2	10
1.2 Autophagy	11
1.2.1 Molecular mechanism of autophagy	12
1.2.2 Xenophagy	14
1.2.3 LC3-associated phagocytosis	15
1.3 <i>Listeria monocytogenes</i>	16
1.3.1 Autophagic targeting of <i>Listeria monocytogenes</i>	17
1.4 Aim of this work	20
2 Materials and Methods	21
2.1 Materials	21
2.1.1 Chemicals, Buffers and Solutions	21
2.1.2 Media and Additives	23
2.1.3 Antibodies	24
2.1.4 Consumable Material	26
2.1.5 Equipment and Devices	26

2.1.6 Software.....	28
2.1.7 Bacteria.....	28
2.1.8 Mice.....	28
2.2 Methods.....	32
2.2.1 Cultivation and preparation of <i>Listeria monocytogenes</i>	32
2.2.2 Isolation and purification of macrophages.....	34
2.2.3 Flow cytometry analysis of peritoneal cells.....	35
2.2.4 Immunofluorescence microscopy.....	36
2.2.5 Western Blot analysis.....	38
2.2.6 ASMase activity assay.....	40
2.2.7 Transmission electron microscopy.....	40
2.2.8 Analysis of survival of infected mice and bacterial burden.....	41
2.2.9 Quantification of ROS.....	41
3 Results.....	42
3.1 L.m. primarily infects F4/80 ⁺ macrophages after intraperitoneal injection.....	42
3.2 LC3 recruitment to L.m.-containing phagosomes is independent of listerial virulence factors.....	44
3.3 Canonical autophagy is not involved in LC3 recruitment to L.m.-containing phagosomes.....	46
3.4 LC3 is recruited to L.m.-containing phagosomes by LC3- associated phagocytosis.....	48
3.5 Mac-1 is the pattern recognition receptor inducing ROS production by Nox2 and LAP in L.m.-infected macrophages.....	52

3.6 Mac-1 induces ROS production by Nox2 and LAP through activation of acid sphingomyelinase.....	54
3.7 LAP increases fusion of L.m.-containing phagosomes with lysosomes.....	56
3.8 LAP contributes to anti-listerial immunity <i>in vivo</i>	60
3.9 Activation of LAP via Mac-1 and ASMase enhances killing of L.m. by promoting phago-lysosomal fusion.....	64
4 Discussion.....	65
5 References.....	72
Summary.....	78
Zusammenfassung.....	79
Danksagung.....	80
Erklärung.....	81
Curriculum vitae.....	82

List of Abbreviations

ActA	Actin assembly-inducing protein
APC	Allophycocyanin
APS	Ammonium persulfate
Arp	Actin-related protein
ASMase	Acid sphingomyelinase
ASMase^{-/-}	Acid sphingomyelinase-deficient
Atg7	Autophagy-related gene 7
Atg7^{MYEL-KO}	Atg7-deficient in myeloid cells
AUC	Area under the curve
BCA	Bicinchoninic acid
BHI	Brain heart infusion
BMDM	Bone marrow-derived macrophages
BSA	Bovine serum albumin
C₁₂FDG	5-Dodecanoylaminofluorescein Di-β-D-galactopyranoside
CD11b	Cluster of differentiation molecule 11B
CD11b^{-/-}	Cluster of differentiation molecule 11B-deficient
CFU	Colony forming units
DMEM	Dulbecco's modified eagle's medium
DMSO	Dimethyl sulfoxide
EDTA	Ethylenediaminetetraacetic acid
ELC	Enhanced chemiluminescence
FACS	Fluorescence activated cell sorting
FCS	Fetal calf serum
Fig.	Figure
GFP	green fluorescent protein
gp91^{phox}	91-kDa glycoprotein component of the phagocyte NADPH oxidase
HBSS	Hank's balanced salt solution

HEPES	4-(2-hydroxyethyl)-1-piperazineethanesulfonic acid
HK L.m.	heat-killed <i>Listeria monocytogenes</i>
HRP	Horseradish peroxidase
IFM	Immunofluorescence microscopy
IgG	Immunoglobulin G
InIK	Internalin K
i.p.	Intraperitoneal
LAP	LC3-associated phagocytosis
LC3	Microtubule-associated protein light chain 3
LLO	Listeriolysin O
L.m.	<i>Listeria monocytogenes</i>
Mac-1	Macrophage 1 antigen
MACS	Magnetic activated cell sorting
M-CSF	Macrophage colony-stimulating factor
min	minutes
MOI	Multiplicity of infection
mTOR	mammalian target of Rapamycin
MVP	Major vault protein
MyD88	Myeloid differentiation primary response gene 88
MyD88^{-/-}	Myeloid differentiation primary response gene 88-deficient
NAC	<i>N</i> -acetyl-L-cysteine
NADPH	nicotinamide adenine dinucleotide phosphate
n.i.	not infected
NMS	normal mouse serum
NOD2	Nucleotide-binding oligomerization domain-containing protein 2
NOD2^{-/-}	Nucleotide-binding oligomerization domain-containing protein 2-deficient
Nox2	NADPH-oxidase 2
Nox2^{-/-}	NADPH-oxidase 2-deficient
n.s.	not significant

PAMP	Pathogen associated molecular pattern
PBS	Phosphate buffered saline
PC-PLC	Phosphatidylcholine-specific phospholipase C
PE (F4/80-PE)	Phycoerythrin
PE (LC3-PE)	Phosphatidylethanolamine
PFA	Paraformaldehyde
p.i.	post infection
PI-PLC	Phosphatidylinositol-specific phospholipase C
PMA	Phorbol-12-myristat-13-acetat
PM	Peritoneal macrophage
RLU	Relative light unit
rpm	revolutions per minute
RT	room temperature
SDS	Sodium dodecyl sulfate
SDS-PAGE	Sodium dodecyl sulfate polyacrylamide gel electrophoresis
SE	Standard error of the mean
SLAP	Spacious Listeria-containing phagosomes
TBS	Tris-buffered saline
TBS-T	Tris-buffered saline and Tween 20
TEM	Transmission electron microscopy
TGS	Tris/Glycine/SDS
TLR2^{-/-}	Toll-like receptor-2-deficient
TRITC	Tetramethylrhodamine
Ub	Ubiquitin
ULK1	Unc-51-like kinase
VLE	Very low endotoxin
Wt	wild-type
ΔActA	Actin assembly-inducing protein-deficient
Δhly	LLO-deficient

1 Introduction

1.1 Macrophages

Macrophages are the first line of defense against intracellular bacteria such as *Listeria monocytogenes* (L.m.). They recognize bacteria by a variety of pattern recognition receptors (PRRs). These receptors recognize conserved bacterial structures referred to as pathogen-associated molecular patterns (PAMPs) as well as damage-associated molecular patterns (DAMPs), which are released in response to stress and tissue damage (Mitchell et al., 2016). Overall, macrophages express almost 200 key receptors that can be subdivided in two classes: the membrane-bound receptors such as Toll-like receptors (TLRs) and the cytosolic receptors e.g. NOD-like receptors (NLRs) (Mitchell et al., 2016; Ley et al., 2016).

As the name indicates, macrophages are specialized in in the uptake (phagocytosis) and degradation of pathogens. After phagocytosis of bacteria, the phagosome undergoes a series of fusion and fission events with early and late endosomes and lysosomes, which finally leads to the formation of a phagolysosome. The phagolysosome is a highly bactericidal organelle, which restricts access of the bacteria to essential nutrients such as iron or amino acids. In addition, the NADPH oxidase 2 (Nox2) and the nitric oxide synthase 2 (NOS2) generate reactive oxygen species (ROS) and reactive nitrogen species (RNS), respectively, which are toxic anti-microbial effectors (Weiss and Schaible 2015; Mitchell et al., 2016). Moreover, upon fusion with lysosomes, enzymes such as acid hydrolases, which target carbohydrates and lipids of the bacteria, thereby destroying its integrity, are delivered into the lumen of the phagosome. In the case of *Listeria monocytogenes*, the transfer of lysosomal proteases such as cathepsin D into L.m.-containing phagosomes is of critical importance for killing of L.m. by macrophages (del Cerro-Vadillo et al., 2006; Schramm et al., 2008).

In addition to the phago-lysosomal pathway, macrophages possess several other

antibacterial effector mechanisms e. g. production of anti-microbial peptides, release of cytokines, efferocytosis and xenophagy.

1.1.1 Mac-1

An important receptor, which is a central part of this work, is the β_2 integrin macrophage-1 antigen (Mac-1, CR3, integrin $\alpha_M\beta_2$). Mac-1 is a heterodimer of CD11b (α_M) and CD18 (β_2), which is a classical integrin that has a broad recognition specificity. The receptor binds to proteins of the extracellular matrix, coagulation proteins and ICAM-1 and -2 (Ehlers, 2000). In addition, Mac-1 serves as a pattern recognition receptor that recognizes DAMPs such as damage-associated alarmin HMGB1 (Gao et al., 2011) and PAMPs such as LPS from gram-negative bacteria, inactivated C3b and several other microbial ligands (Ehlers, 2000). It is mainly expressed on innate immune cells, such as monocytes, granulocytes, natural killer cells and macrophages. The receptor is involved in several immune cell responses including cell adhesion, migration, phagocytosis, cellular activation, and other (Solovjov et al., 2005).

In the context of L.m. infection, Mac-1 has been shown to be required for killing of L.m. by macrophages (Drevets et al., 1993), however, the underlying molecular mechanisms remain to be elucidated. Another study, which is important for this work, has demonstrated that Mac-1 can mediate activation of Nox2 in macrophages, in response to extracellular dsRNA (Zhou et al., 2013). However, it is not known, whether Mac-1 can mediate activation of Nox2 in response to bacterial infection of macrophages.

1.1.2 Acid sphingomyelinase

Sphingomyelinases catalyze the hydrolysis of sphingomyelin to phosphorylcholine and ceramide. To date, a family of at least seven different sphingomyelinases has been described in mammalian cells, tissues and biological fluids (Levade and Jaffrezou 1999). They can be classified according their optimal pH range: alkaline, neutral and acid sphingomyelinases.

Acid sphingomyelinase (ASMase) has its optimum activity at pH 4.5 - 5.0 and has been detected in almost all cell types that have been studied, including macrophages. It localizes to the luminal leaflet of phagosomes, lysosomes, endosomes, and to the extracellular leaflet of plasma membranes. Due to its optimal activity at acidic pH, ASMase has been characterized as a lysosomal protein. Nevertheless, a secreted form of ASMase (secretory ASMase) has also been described (Truman, Al Gadban et al. 2011).

Upon activation signaling, the secretory vesicles containing ASMase are mobilized to fuse with the extracellular leaflet of the plasma membrane. Plasma membranes primary consist of sphingolipids and the most common shingolipid is sphingomyelin, which is the substrate of ASMase. The generation of ceramide by ASMase within certain membrane areas, alters the biophysical properties of these membrane domains. For example, the tension in luminal leaflets of vesicles is increased, which results in bending of the membrane and thereby enables an efficient fusion with other membrane-bound vesicles or with the plasma membrane (Gulbins and Li 2006; Utermohlen, Herz et al. 2008).

In the context of L.m. infection, it was shown that ASMase deficient mice are highly susceptible to infection with *Listeria monocytogenes*. Despite activation, ASMase^{-/-} macrophages cannot inactivate and eliminate phagocytosed L.m. (Utermohlen, Karow et al. 2003). The reason for this is that in ASMase^{-/-} macrophages the fusion of lysosomes with phagosomes is impaired. Consequently lysosomal hydrolases, which are responsible for the

degradation of phagocytosed listeria, cannot be delivered effectively to the phagosome (Schramm, Herz et al. 2008).

Apart from that, it was shown that in the context of *Pseudomonas aeruginosa* infection of macrophages, generation of ceramide-enriched membrane platforms by ASMase is important for activation of Nox2 (Zhang et al., 2008). Nevertheless, the mechanism by which *P. aeruginosa* stimulates ASMase and subsequent ROS release by Nox2 remains to be elucidated.

1.1.3 NADPH oxidase 2

The members of the family of NADPH oxidases are the primary source of regulated production of reactive oxygen species in a wide range of cell types and organisms. In humans, there are seven members of the Nox family of NADPH oxidases, which consists of consists of Nox1, Nox2, Nox3, Nox4, Nox5, Duox1, and Duox2. All these Nox and Duox isoforms are also present in mice, except for Nox5 (Bedard and Krause, 2007).

The Nox isoforms have multiple functions, which are important for normal physiology e.g. vasoregulation, hormone synthesis, regulation of gene expression, cell proliferation and differentiation. By contrast, Nox2, which is mainly expressed in professional phagocytes including neutrophils, dendritic cells and macrophages, is a crucial player in antimicrobial immunity (Singel and Segal, 2016).

Nox2 consists of a membrane-bound heterodimer, comprised of gp91^{phox} and p22^{phox} and cytoplasmic subunits p40^{phox}, p47^{phox}, p67^{phox} and Rac. Upon activation, which can be triggered by binding of different PAMPs to specific pathogen recognition receptors, or through integrin-dependent adhesion, the cytoplasmic subunits translocate to the membrane-bound heterodimer (Singel and Segal, 2016).

The active Nox2 complex converts molecular oxygen to superoxide anion (O_2^-), which can be further converted to other downstream reactive oxygen species with antimicrobial activity e. g. H_2O_2 . Macrophages, which have a mutation in the membrane-bound subunit gp91^{phox}, show increased susceptibility to mycobacterial infections (Bustamante et al., 2011). Despite the important role of Nox2 in anti-microbial immunity, there is now growing evidence that Nox2 ROS can also influence different cellular signaling pathways (Holmström and Finkel, 2014). Specifically, Nox2-generated ROS have been shown to regulate antibacterial autophagy in human epithelial cells (Huang et al., 2009). In the context of L.m. infection, a more recent publication has demonstrated that production of ROS by Nox2 is necessary for LC3 recruitment of the microtubule-associated protein light chain 3 (LC3) to L.m.-containing phagosomes (Lam et al., 2013). Nevertheless, the molecular mechanisms by which L.m. trigger ROS production and subsequent LC3 recruitment, remains elusive.

1.2 Autophagy

For the maintenance of cellular homeostasis, new proteins must be constantly synthesized and aged, misfolded, or redundant proteins as well as damaged or aged organelles must be removed. The equilibrium between *de novo* synthesis and degradation is tightly regulated by different mechanisms, in response to environmental conditions. Under starvation conditions, protein synthesis is restricted due to the lack of nutrients; therefore dispensable proteins are degraded in order to regain nutrients. The degradation of proteins is either performed by proteasomes or lysosomes. While proteasomes do only degrade proteins, lysosomes are also able to degrade whole organelles. The major pathway, by which substrate prone for degradation is delivered to the lysosome, is autophagy (Wang and Klionsky 2003).

In eukaryotic cells, three major autophagic pathways being involved in lysosomal degradation are distinguished: Chaperone-mediated autophagy, microautophagy and

macroautophagy. In chaperone-mediated autophagy, chaperons e. g. Hsc70 transport unfolded, cytosolic proteins directly across the lysosomal membrane into the lysosome. Microautophagy is involved in the engulfment of small portions of the cytoplasm, directly at the surface of the lysosome. During macroautophagy – here referred to as autophagy – protein cargo together with portions of the cytosol are sequestered into a double-membrane compartment termed as autophagosome. Upon fusion with endosomes and lysosomes, autophagosomes mature into autolysosomes, in which the substrate is degraded by lysosomal enzymes, e. g. acid hydrolases. (Yang and Klionsky 2010).

1.2.1 Molecular mechanism of autophagy

Autophagy can be induced by several conditions or signals, such as starvation, growth factor deprivation, energy depletion or immune signals. The initiation of autophagy starts with the formation of a cup-shaped double membrane structure (Fig. 1), termed the phagophore (Levine, Mizushima et al. 2011). According to current knowledge the isolation membrane, from which the phagophore is formed, originates at the endoplasmic reticulum, particularly at the mitochondria contact sites (Hamasaki, Furuta et al. 2013). In most cases, autophagy induction is regulated by the unc-51-like kinase (ULK1). Under nutrient-rich conditions, ULK1 is phosphorylated by the mammalian target of Rapamycin (mTOR), thereby autophagy induction is inhibited. Upon starvation, the mTOR complex dissociates from ULK1, which results in autophagy induction (Wong, Puente et al. 2013). mTOR can be also pharmacologically inhibited using Rapamycin, which also results in autophagy induction (Brown, Albers et al. 1994). Downstream of ULK1, the elongation of the phagophore is regulated by different ubiquitin-like conjugation systems and autophagy-related genes (Atg) (Wong, Puente et al. 2013).

The microtubule-associated protein light chain 3 (LC3) plays an essential role in this elongation process. Initially, cytosolic ProLC3 is cleaved by Atg4, resulting in the formation of LC3-I. Subsequently LC3-I is conjugated to phosphatidylethanolamine (PE) by Atg3, resulting in the formation of LC3-II. Finally, LC3-II is targeted to the phagophore, where it stimulates the elongation and closure of the autophagosome. Analysis of the conversion of cytosolic LC3-I into membrane-associated LC3-II is an important method to monitor autophagy (Florey and Overholtzer 2012).

Autophagosomes matureate by fusion with endosomes. In the course of these fusion processes, the autophagosome acquires membrane proteins and proton pumps resulting in the formation of an amphisome. During the last maturation step, the outer membrane of the amphisome fuses with lysosomes, forming an autolysosome. Inside the autolysosome the inner membrane of the autolysosome is degraded by lysosomal hydrolases together with its cargo (Eskelinen and Saftig 2009; and Fig. 1). The degraded products are transported back to the cytoplasm and can be reused for protein synthesis or energy generation.

Figure 1

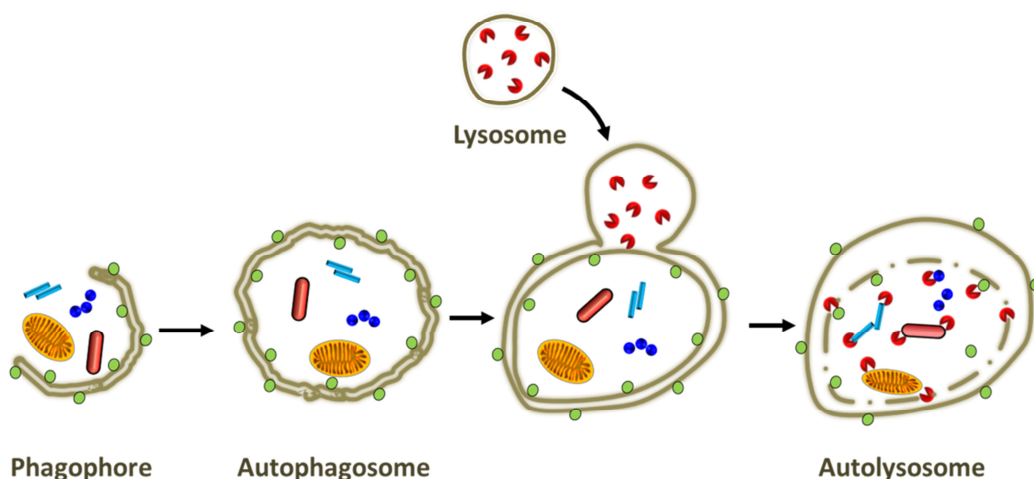


Figure 1: Schematic representation of the autophagy process.

The autophagy process is initiated by the formation of the isolation membrane termed the phagophore. The phagophore expands and sequesters its cargo. The closure of the phagophore results in the formation of double membrane-bound autophagosome. The fusion of the autophagosome with lysosomes results in the formation of the autolysosome, in which the cargo is degraded by lysosomal enzymes.

Finally, the autolysosome becomes a lysosome and can undergo a further fusion with autophagosomes or amphisomes. If the substrate cannot be degraded completely, the autolysosome becomes a residual body containing indigestible material (Eskelinen and Saftig 2009).

1.2.2 Xenophagy

Beyond the above described housekeeping function, autophagy is involved in innate and adaptive immune responses against intracellular pathogens. In particular, the autophagic machinery can selectively target cytosolic pathogens for sequestration within autophagosomes (Huang and Brumell, 2014). Since microbes are foreign material, the autophagic process by which pathogens are delivered to lysosomes for degradation, is correctly termed xenophagy, but for the sake of better understanding it will be referred to as autophagy.

Various pathogens have adapted specific strategies to avoid their recognition and subsequent targeting to the autophagic machinery for degradation. One of these strategies is exerted by *Brucella abortus* and *Legionella pneumophila*, which can inhibit the maturation of the autophagosome through inhibition of lysosome fusion. This strategy leads to the formation of a bacteria-containing vacuole, which can result in a persistent infection (Yuk, Yoshimori et al. 2012). A different strategy is used by *Shigella flexneri*, which can block autophagic targeting through the secretion of the effector protein *icsB*. *IcsB* prevents the binding of Atg5 to the bacterial surface and thereby evades assimilation into the autophagosome (Ogawa, Yoshimori et al. 2005). A further strategy is applied by *Listeria monocytogenes*, which escape from the phagosome into the cytoplasm by secretion of pore-forming lysins and subsequently disguise themselves as subcellular organelles by recruitment of host proteins to the bacterial surface (Lerena, Vazquez et al. 2010).

1.2.3 LC3-associated phagocytosis

Recently several studies have shown that LC3, which is widely used as an autophagy marker, can be recruited to single-membrane phagosomes. This process, which cannot be easily distinguished from canonical autophagy, is termed LC3-associated phagocytosis (LAP). The most important examples for LAP, (also referred to as non-canonical autophagy), are summarized below.

As one of the first, the lab of Douglas Green has shown that LC3 is recruited to phagosomes containing particles that engage TLRs or during the engulfment of dead cells (Sanjuan et al. 2007; Martinez et al. 2011). Another study described that LC3 can be recruited to fungi-containing phagosomes, which is dependent on the surface receptor Dectin-1 (Becker et al. 2012; Tam et al. 2014). LC3 can be also recruited to bacteria-containing phagosomes, which has been shown for *Burkholderia pseudomallei* (Gong et al. 2011), *Listeria monocytogenes* (Lam et al. 2013), *Shigella flexneri* (Baxt and Goldberg 2014), *Yersinia pseudotuberculosis* (Ligeon et al. 2014), *Legionella dumoffii* (Hubber et al. 2017) and *Mycobacterium tuberculosis* (Köster et al. 2017). In addition, LC3 has been also shown to be recruited to endolysosomes, which can be triggered by osmotic imbalances caused by lysosomotropic drugs (Florey et al. 2015).

Mechanistically, LAP, is a process which requires some components of the autophagic machinery (e.g. Atg5, Atg7 and Beclin-1) but is independent of others (e.g. Ulk complex components, i.e. Ulk1/2, FIP200, Atg13 and Atg101) (Martinez et al., 2015). A hallmark of LAP is the recruitment of LC3 to single-membrane phagosomes which requires production of reactive oxygen species by Nox2 (Huang et al., 2009). LAP has been shown to be involved in various cellular processes such as phagosomal maturation and microbial killing but also suppression of pro-inflammatory signals or MHC class II antigen presentation (Mehta et al., 2014). However, the underlying molecular mechanisms remain to be elucidated.

1.3 *Listeria monocytogenes*

Listeria monocytogenes is a gram-positive, rod-shaped bacterium with variable lifestyle. It can survive in soil, in water and as saprophyte at vegetation or as a facultative intracellular pathogen in a wide range of host species. Humans usually take up listeria via consumption of contaminated food. Therefore, the primary route of infection is the gastrointestinal epithelium. Listeria enter the host's intestinal epithelial cells through the exploitation of the host endocytic machinery. Inside host cells, listeria escape from the phagosomes by secretion of a pore-forming toxin listeriolysin O. Upon phagosomal escape, listeria switch their metabolism and become an intracellular pathogen (Freitag, Port et al. 2009; Ray, Marteyn et al. 2009). Within the cytoplasm, listeria activate components of host's cellular actin assembly machinery and induce the formation of actin tails on their surface. Polymerization of actin provides a motility force that propels the bacteria through the cell cytoplasm and also enables entry into adjacent cells (Goldberg 2001).

After entry into the blood stream, most of the listeria end up in the liver and spleen. In healthy individuals listeria infection can result in a self-limiting gastroenteritis. However, immunocompromised individuals are at risk to develop a meningitis or encephalitis. In pregnant woman, an infection of the developing fetus can result in abortion or stillbirth (Freitag, Port et al. 2009; Ray, Marteyn et al. 2009).

1.3.1 Autophagic targeting of *Listeria monocytogenes*

Listeria monocytogenes enter non-phagocytic cells, such as epithelial cells or hepatocytes by internalin-mediated endocytosis. Additionally, listeria are phagocytosed by professional phagocytes, such as macrophages. Inside the host cell, listeria escape from the phagosome by the secretion of the pore-forming toxin listeriolysin O (LLO) and two phospholipases PI-PLC and PC-PLC. It was reported that LLO can induce autophagy via the Ub-p62-LC3 pathway (Ogawa, Yoshikawa et al. 2011). Thereby, either LLO itself or membrane remnants of the phagosome as well as cytosolic listeria can become ubiquitinated. Via the adaptor molecule p62, the ubiquitinated cargo is linked to LC3 and subsequently targeted to the phagophore (Ogawa, Yoshikawa et al. 2011; and Fig. 2 B).

A different pathway was described by Meyer-Morse et al. in 2010. These authors reported that the invasive process of listeria is recognized via NOD1-Atg16L-LC3 pathway, which involves the intracellular pattern recognition receptor NOD1 (Meyer-Morse, Robbins et al. 2010). In addition, Anand et al. reported in 2011 that autophagy of *L. monocytogenes* is dependent on extracellular signal-regulated kinase (ERK), which involves TLR-2 and NOD2 signaling (Anand, Tait et al. 2011). A recent study showed that LC3 can be directly recruited to the single-membrane phagosome by LC3-associated phagocytosis pathway, which is dependent on the NADPH oxidase 2 (Nox2) (Lam, Cemma et al. 2013; and Fig. 2 A). Nevertheless, the mechanisms of this pathway have not been fully elucidated and several questions remain unclear.

Figure 2

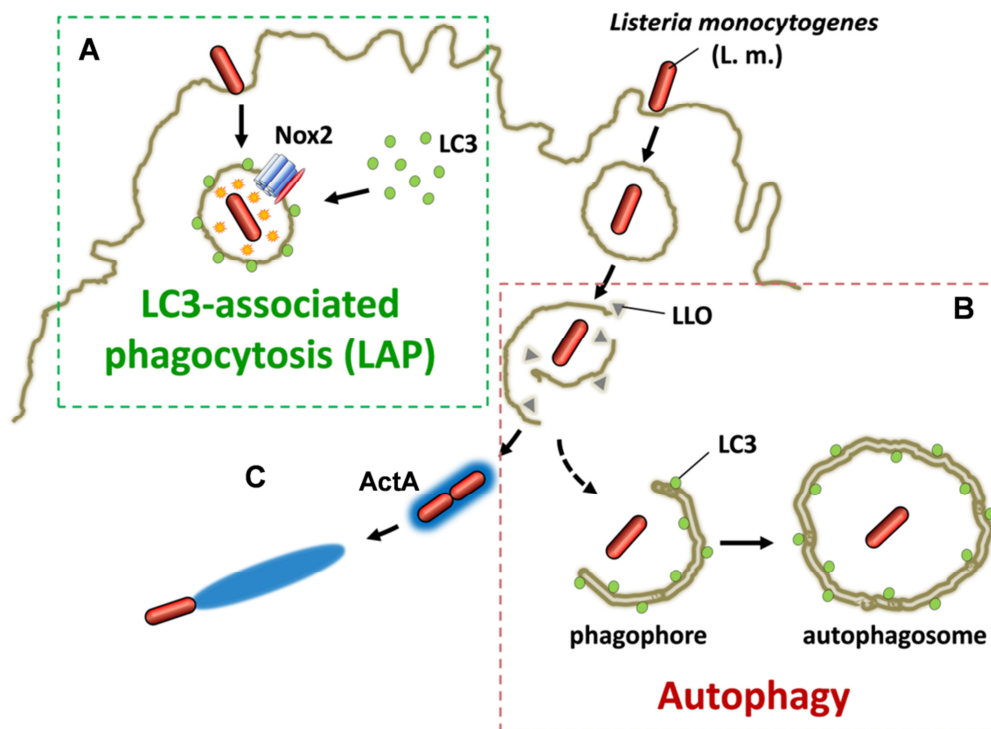


Figure 2: Autophagic targeting of *Listeria monocytogenes*.

- (A) LC3-associated phagocytosis: Production of reactive oxygen species (ROS) by the NADPH oxidase 2 (Nox2), triggers LC3 recruitment to the L.m.-containing phagosome.
- (B) Autophagy: L.m. escapes from the phagosome by secretion of listeriolysin O. Membrane remnants from the lysed phagosome, the damaged phagosome itself or cytosolic L.m. can be targeted by canonical autophagy. Thereby, the phagophore expands and sequesters the listeria, resulting in the formation of a double-membrane autophagosome.
- (C) L.m. subverts autophagic recognition by ActA-mediated camouflage and induces actin polymerization for motility

Similar to the variety of different autophagy pathways, several strategies to avoid autophagic recognition and subsequent degradation in the lysosome have been described for *Listeria monocytogenes*. The best studied mechanism is the ActA-mediated camouflage, which prevents autophagic recognition. Upon escape from the phagosome, listeria expresses an actin assembly-inducing protein (ActA), which has two different functions. First, ActA interacts with host actin-related protein complex 2/3 (Arp2/3) and actin monomers to induce actin polymerization. This enables actin-based motility (Yoshikawa, Ogawa et al. 2009; and Fig. 2 C). Second, recruitment of Arp2/3, VASP (vasodilator-stimulated phosphoprotein) and actin to the bacterial surface by ActA disguises the bacterium as a subcellular organelle.

Thus, ubiquitination of the bacteria and subsequent autophagic targeting via Ub-p62-LC3 pathway is prevented (Yoshikawa, Ogawa et al. 2009). A similar camouflage strategy is the recruitment of the major vault protein (MVP) by Internalin K (InlK). Thereby the bacterial surface is decorated with MVP, which also prevents autophagic recognition (Dortet, Mostowy et al. 2011). A different strategy to overcome lysosomal degradation is the prevention of phagosomal maturation. By constant low-level expression of LLO, listeria prevents the fusion of phagosomes with lysosomes and slowly proliferates in spacious Listeria-containing phagosomes (SLAPs) (Birmingham, Canadien et al. 2008).

Summarizing, data on the role of autophagy in immunity to L.m. are controversial. On the one hand, autophagy has been shown *in vitro* to target and degrade L.m. early after infection (Py et al., 2007) and to be required for *in vivo* control of L.m. infection in *Drosophila melanogaster* (Yano et al., 2008) and *Tenebrio molitor* (Tindwa et al., 2015). On the other hand, L.m. has been reported to avoid autophagy by multiple mechanisms (Huang and Brumell, 2014). While defective autophagy in myeloid cells leads to enhanced susceptibility of mice to L.m. infection (Zhao et al., 2008), L.m. has also been reported to exploit the autophagic machinery to form a replicative niche in macrophages (Birmingham et al., 2008; Lam et al., 2013).

So far, detailed *in vivo* data from mammals on the role of autophagy and LAP in immunity to L.m. are largely missing. Specifically, it remains unclear if the autophagic machinery can target L.m. or if virulent L.m. avoid autophagic targeting. Also, it remains an open question if autophagy and/or LAP contribute to anti-listerial immunity or provide L.m. with a replicative niche for persistent infection.

1.4 Aim of this work

Data on autophagic targeting of L.m. are controversial. In particular, *in vivo* data from mammals on the roles of autophagy and LAP in immunity to L.m. are largely missing. Moreover, the molecular mechanisms leading to initiation of LAP in response to L.m. infection remain completely unknown.

The aim of this study is to delineate the molecular mechanisms underlying autophagic targeting of L.m. *in vivo* and to solve the question whether canonical autophagy and/or LAP contribute to anti-listerial immunity or rather provide L.m. with a replicative niche for persistent infection.

2 Materials and Methods

2.1 Materials

All buffers and solutions were prepared with de-ionized water (bidest. H₂O) from an EASYpure UV/UF H₂O purification unit (Werner Reinstwassersysteme, Leverkusen). To sterilize solutions they were either autoclaved or sterile filtrated using 0.2 µm filters. All buffers and solutions were stored at room temperature unless specified otherwise.

2.1.1 Chemicals, Buffers and Solutions

Substance	Chemical composition/Manufacturer
Acrylamide 4K-Solution (40%) Mix	AppliChem, stored at 2-8° C
Amersham ELC Detection reagents	GE Healthcare, stored at 2-8° C
APS	Sigma-Aldrich
BCA Protein Assay Kit	Thermo Scientific
Benzonase	Novagen, stored at -20° C
Blocking solution (milk)	5 % powdered milk in TBS-T, stored at -20° C
Blocking solution (BSA)	5 % BSA in TBS-T, stored at -20° C
BSA	Sigma-Aldrich, stored at 2-8° C
BSA blocking solution	3 % BSA in PBS, stored at 2-8° C
C ₁₂ FDG	Molecular Probes, stored at -20° C
CD11b MicroBeads	Miltenyi Biotec, stored at 2-8° C
Chloroquine	Sigma-Aldrich, stored at 2-8° C
DAPI	Sigma-Aldrich, stored at -20° C
Deoxycholic acid	Sigma-Aldrich
DMSO	Merck Millipore
EDTA	Carl Roth GmbH & Co. KG

FACS Fix	2.5 % formaldehyde, 1 % FCS in PBS
FluoSpheres (1 μm)	Molecular Probes, stored at 2-8° C
FluoSpheres (0.02 μm)	Molecular Probes, stored at 2-8° C
High-Range Rainbow Mol. Weight Marker	GE Healthcare, stored at -20° C
IFN- γ	R&D Systems, stored at -20° C
Laemmli buffer (5 x)	60 mM Tris/HCl, 25 % Glycerol, 10 % β -mercaptoethanol, 2 % SDS, 0,2 % bromphenol blue in H ₂ O, stored at -20° C
LumiGLO Reserve Chemiluminiscent substr.	KPL Inc
MACS buffer	0.5 % BSA, 200 mM EDTA in PBS
NAC	Sigma-Aldrich, stored at 2-8° C
NaCl lysis buffer (0.2 %)	0.2 % NaCl in H ₂ O, stored at 2-8° C
NaCl lysis buffer (1.6 %)	1.6 % NaCl in H ₂ O, stored at 2-8° C
NH ₄ Cl/Tris lysis buffer	8.3 % NH ₄ Cl, 0.1 M Tris in H ₂ O, stored at 2-8° C
Nonidet P40	Sigma-Aldrich
PageRuler Prestained Protein Ladder	Thermo Scientific, stored at -20° C
Paraformaldehyde solution	3 % PFA in PBS, stored at -20° C
Penicillin / Streptomycin	Penicillin (10000 U/mL) and Streptomycin (10 ng/mL) in H ₂ O, Biochrom AG, stored at 2-8° C
Phalloidin	Molecular probes, stored at -20° C
Phorbol 12-myristate 13-acetate (PMA)	Sigma-Aldrich, stored at -20° C
Phosphatase inhibitors	Roche, stored at 2-8° C
Powdered milk	Carl Roth GmbH & Co. KG
ProLong Gold antifade reagent	Invitrogen, stored at -20° C
Protease inhibitors	Roche
Rapamycin	LC Laboratories, stored at -20° C
RIPA buffer	150 mM NaCl, 50 mM TrisHCl, 1 % SDS, 0.5 % Nonidet P40, 0.1 % deoxicollic acid
Rotenone	Sigma-Aldrich, stored at -20° C

Roti-Blot A anode buffer (10 x)	Carl Roth GmbH & Co. KG
Roti-Blot K cathode buffer (10 x)	Carl Roth GmbH & Co. KG
Saponin from quillaja bark	Sigma-Aldrich
Saponin blocking buffer	0.1 % Saponin, 3 % BSA in PBS
Saponin washing buffer	0.1 % Saponin in PBS
SDS	AppliChem
NaCl	AppliChem
TBS	150 mM NaCl, 10 mM Tris-HCl in H ₂ O
TBS-T	0.1 % Tween 20 in TBS
TEMED	AppliChem, stored at 2-8° C
Tetramethylrhodamine isothiocyanate Isomer R (TRITC)	Sigma-Aldrich, stored at -20° C
TGS buffer (10 x)	Bio-Rad Laboratories, Inc.
TNF (mouse, recombinant)	R&D Systems, Inc. stored at 2-8° C
TrisHCl buffer (0.5 M and 1.5 M)	Bio-Rad Laboratories, Inc.
Triton X-100	Sigma-Aldrich
Trypan blue solution	Sigma-Aldrich
Tween 20	AppliChem
2-propanol	Carl Roth GmbH & Co. KG

2.1.2 Media and Additives

<u>Name of substance</u>	<u>Manufacturer/Distributor</u>
BHI medium	Becton Dickinson GmbH
Dulbecco's MEM (1 x)	Biochrom AG, stored at 2-8° C
FCS (fetal calf serum)	Biowest, stored at -20° C
HBSS	Life technologies, stored at 2-8° C
HEPES-Buffer (1 M)	Biochrom AG, stored at 2-8° C

M-CSF	PeptoTech, stored at -20° C
NMS (CD-1 mouse complement serum)	Innovative Research, Inc., -20° C
PBS Dulbecco (1 x)	Biochrom AG, stored at 2-8° C
Sodium Pyruvate (100 mM)	Biochrom AG, stored at 2-8° C
VLE RPMI 1640	Biochrom AG, stored at 2-8° C

2.1.3 Antibodies

FACS Antibodies

<u>Antigen</u>	<u>Specification /Provider</u>
CD16/CD32	purified rat-anti-mouse CD16/CD32 (mouse Fc receptor Block), BD Biosciences, stored at 4° C
Ly6C	Rat-anti-mouse Ly-6C APC antibody, APC-conjugated, eBioscience, stored at 4° C
Ly6C	Rat-anti-mouse Ly-6C antibody, FITC-conjugated, BD Biosciences, stored at 4° C
Ly6G	Rat-anti-mouse Ly-6G (Gr-1), PE-conjugated, eBioscience, stored at 4° C
Ly6G	Rat-anti-mouse Ly-6G antibody, FITC-conjugated, BD Biosciences, stored at 4° C
F4/80	Rat-anti-mouse F4/80 antibody, APC-conjugated, eBioscience, stored at 4° C
F4/80	Rat-anti-mouse F4/80 antibody, PE-conjugated, eBioscience, stored at 4° C
CD11b	Rat-anti-mouse CD11b antibody, APC-conjugated, BD Biosciences, stored at 4° C
CD11b	Rat-anti-mouse CD11b antibody, PE-conjugated, BD Biosciences, stored at 4° C
CD45R FITC	Rat-anti-human/mouse CD45R (B220) antibody, FITC-conjugated, eBioscience, stored at 4° C
Gr-1	Rat-anti-mouse Ly-6G and LY-6C antibody, FITC-conjugated, BD Biosciences, stored at 4° C

Western Blot Antibodies

Antigen	Specification /Provider
β -actin	monoclonal mouse-anti- β -actin antibody, Sigma-Aldrich, stored at 2-8°C
LC3B	polyclonal rabbit-anti-LC3B antibody, Sigma-Aldrich, stored at 2-8° C
Mouse IgG	goat-anti-mouse antibody, HRP-conjugated, Sigma-Aldrich, stored at 2-8° C
Rabbit IgG	goat-anti-rabbit antibody, HRP-conjugated, Sigma-Aldrich, stored at 2-8° C
phospho-p70 S6 Kinase	Rabbit-anti-phospho-p70 S6 Kinase antibody, Cell Signaling, stored at -20° C
p70 S6 Kinase	Rabbit-anti-p70 S6 Kinase antibody, Cell Signaling, stored at -20° C
phospho-p40 ^{phox}	Rabbit-anti-phospho-p40 ^{phox} antibody, Cell Signaling, stored at -20° C

Microscopy Antibodies

Antigen	Specification /Provider
<i>L. monocytogenes</i>	purified polyclonal rabbit anti-L.monocytogenes antibody, US Biologicals, stored at 2-8° C
Rabbit IgG	goat-anti-rabbit antibody, AlexaFluor 405-conjugated, Molecular Probes, stored at 2-8° C
Rabbit IgG	goat-anti-rabbit antibody, AlexaFluor 488-conjugated, Molecular Probes, stored at 2-8° C
Rabbit IgG	goat-anti-rabbit antibody, AlexaFluor 568-conjugated, Molecular Probes, stored at 2-8° C
Rabbit IgG	goat-anti-rabbit antibody, AlexaFluor 647-conjugated, Molecular Probes, stored at 2-8° C
LC3	mouse-anti-LC3 antibody, MBL, stored at -20° C
Mouse IgG	goat-anti-mouse antibody, AlexaFluor 488-conjugated, Molecular Probes, stored at 2-8° C

2.1.4 Consumable Material

<u>Name</u>	<u>Manufacturer/Distributor</u>
Amersham Hyperfilm ECL	GE Healthcare
BD Microlance 3 Needles	Becton Dickinson GmbH
Blood agar plates	Oxoid Deutschland GmbH
Cover glass (Ø 13 mm)	VWR International
Criterion Empty Cassettes	Bio-Rad Laboratories, Inc.
FACS tubes (5 mL)	BD Biosciences
Falcon tubes (15 and 50 mL)	Greiner Bio-One
gentleMACS M tubes	Miltenyi Biotec
MACS Separation Columns (LS)	Miltenyi Biotec, stored at 2-8° C
Microscope slides	Engelbrecht
Omnifix Syringes (3, 5 and 10 mL)	B. Braun
Parafilm	American National Can
Pipette tips (5, 10 and 25 mL)	Sarstedt
Tissue Culture plates	TPP
Whatman 3 mm (filter paper)	GE Healthcare
Whatman Nitrocellulose membrane	GE Healthcare

2.1.5 Equipment and Devices

<u>Device</u>	<u>Specification</u>	<u>Manufacturer/ Distributor</u>
Automatic colony counter	Flash & Go	IUL S. A.
Balance	Sartorius L2200P	Gemini B. V.
Cell counting chamber	Neubauer Improved	LO Laboroptik
Centrifuges	Heraeus Multifuge 4KR	Thermo Scientific
	Eppendorf 5417R	Thermo Scientific

CO ₂ incubator	Heraeus Hera cell 240	Thermo Scientific
Confocal laser scanning microscope	FluoView 1000	Olympus Corporation
Developing machine	Aqfa Curix 60	AGFA HealthCare
Electrophoresis cell	Criterion Cell	Bio-Rad Laboratories, Inc.
Flow cytometer	FACSCalibur	BD Biosciences
Fluorescence microscope	IX81	Olympus
Imaging system	MF-ChemiBIS 3.2	DNR Bio Imaging Systems
Incubator	Kelvitron T	Heraeus Instruments GmbH
Incubator shaker	Innova 4200	New Brunswick Scientific
Laminar flow hood	HERAsafe KS	Thermo Scientific
	HERAsafe	Thermo Scientific
Magnetic mixer	RCT basic	Kika Labortechnik
Microcentrifuge	GalaxyMiniStar	VWR International
Magnetic separator	QuadroMACS	Miltenyi Biotec
Microscope	Axiovert 25	Carl Zeiss MicroImaging
Microtiterplate-reader	Tecan infinite M1000	Tecan Group Ltd.
Multimode plate reader	Tristar2 LB 942	Berthold Technologies
Photometer	Eppendorf Bio	Thermo Scientific
Power Supply	Power Pac 3000	Bio-Rad Laboratories, Inc.
Protein blotting system	Trans-Blot Turbo	Bio-Rad Laboratories, Inc.
Shaker	Titramax 101	Heidolph
Spiral plater	Eddy Jet	IUL S. A.
Thermomixer	Eppendorf comfort	Thermo Scientific
Tissue dissociator	gentleMACS	Miltenyi Biotec
Tumbling table	Biometra WT 12	Biometra GmbH
Vacuum gas pump	VP 86	VWR International
Vortex	Omnilab REAX 2000	Heidolph

2.1.6 Software

<u>Name</u>	<u>Manufacturer/Distributor</u>
Cell Quest Pro	BD Biosciences
Flash & Go 1.2	IUL S. A.
Fluoview FV10 ASW 1.7b	Olympus Corporation
GelCapture 7.0	DNR Bio Imaging Systems Ltd.
GraphPad Prism 5.04	GraphPad Software, Inc.
ImageJ 1.46h	Wayne Rasband
Office Professional Plus 2010	Microsoft
Photoshop CS3	Adobe
SigmaPlot 13.0	Systat Software, Inc.
Tecan i-control 1.7	Tecan Group Ltd.

2.1.7 Bacteria

Listeria monocytogenes, strain EGD-e (serotype 1/2a), were kindly provided by C. Kocks (Harvard Medical School, Boston, USA). The isogenic *L. monocytogenes* deletion mutants Δ prfA, Δ hly and Δ ActA (Peters, Domann et al. 2003) were kindly provided by Eugen Domann (University of Giessen, Germany).

2.1.8 Mice

All mice were heterozygously backcrossed to the C57BL/6 strain to the 10th generation. The animals were bred under specific pathogen-free conditions at the animal facilities of the Medical Centre of the University of Cologne (Cologne, Germany). Homozygous transgenic knock-out mice and corresponding wild-type littermates, at least 6 weeks old, were used for experiments.

All experiments were performed in accordance with the Animal Protection Law of Germany and in compliance with the Ethics Committee at the University of Cologne.

ASMase^{-/-} mice

ASMase-deficient mice (Horinouchi, Erlich et al. 1995) were originally generated by E. H. Schuchmann (Mount Sinai School of Medicine, New York). Breeding pairs of mice heterozygously deficient for acid sphingomyelinase were kindly provided by R. Kolesnick (Memorial Sloan-Kettering Cancer Center, New York).

Atg7^{MYEL-KO} mice

Atg7^{MYEL-KO} mice were generated by crossing Atg7^{fl/fl} mice (purchased from The Jackson Laboratory) to mice expressing the Cre recombinase under the lysozyme M promotor (Clausen, Burkhardt et al. 1999).

CD11b^{-/-} mice

CD11b-deficient mice (purchased from The Jackson Laboratory) were kindly provided by Martin Mollenhauer (Uniklinik Köln, Germany).

FIP200^{MYEL-KO} mice

FIP200^{MYEL-KO} mice were generated by crossing FIP200^{fl/fl} mice (Gan et al., 2006) (a kind gift of Jun-Lin Guang, University of Cincinnati, USA) to mice expressing the Cre recombinase under the lysozyme M promotor.

GFP-LC3-transgenic mice

Breeding pairs of mice heterozygously transgenic for GFP-LC3 (Mizushima, Yamamoto et al. 2004) were kindly provided by Noboru Mizushima (National Institute for Basic Biology, Okazaki, Japan).

MyD88^{-/-} mice

MyD88-deficient mice were a kind gift of Manolis Pasparakis (University of Cologne, Cologne, Germany).

NOD2^{-/-} mice

NOD2-deficient mice were commercially purchased from The Jackson Laboratory (Bar Harbor, USA)

Nox1^{-/-} mice

Nox1-deficient mice (Gavazzi, Banfi et al. 2006) were a kind gift of Karl-Heinz Krause (University of Geneva, Geneva, Switzerland).

Nox2^{-/-} mice

Nox2-deficient mice (Pollock, Williams et al. 1995) were a kind gift of Ralph P. Brandes (Goethe-University, Frankfurt, Germany).

Nox4^{-/-} mice

Nox4-deficient mice (Carnesecchi, Deffert et al. 2011) were a kind gift of Ralph P. Brandes (Goethe-University, Frankfurt, Germany).

TLR2^{-/-} mice

TLR2-deficient mice were commercially purchased from The Jackson Laboratory (Bar Harbor, USA)

2.2 Methods

All cells were incubated at 37° C in CO₂ incubator (5 %) without antibiotics in Dulbecco's modified eagle's medium (DMEM), which was supplemented with 10% heat-inactivated FCS, unless otherwise specified. All centrifugation steps were performed at 300 x g, at 4° C for 5 min, unless otherwise specified. The statistical analysis of data was performed using either Student's t-test or one way analysis of variances (ANOVA). P values smaller than 0.05 were considered as statistically significant. Data are shown as mean ± standard error of the mean.

2.2.1 Cultivation and preparation of *Listeria monocytogenes*

Cultivation of L.m.

Log-phase cultures of *Listeria monocytogenes*, strain EGD-e (serotype 1/2a) or the isogenic Δ hly or Δ prf-deletion mutants were stored at -80° C. Aliquots of these cultures were taken from the -80° C stock and plated onto blood agar plates. After 12 hours of incubation at 37° C, a single colony from the blood agar plate was transferred into 5 mL BHI medium and incubated over night at 37° C, 220 rpm. On the next day, 1 mL of the over-night culture was transferred into 25 mL pre-warmed BHI medium in Erlenmeyer flask and incubated at 37° C, 220 rpm, until an optical density at 600 nm (OD₆₀₀) of 0.3 was reached. Thereafter, the L.m. culture was transferred into a 50 mL falcon tube and centrifuged for 5 min at 3000 g, 4° C. After centrifugation, the supernatant was discarded and the pellet was washed with 10 mL cold PBS. After a second centrifugation step, the pellet was resuspended in 1 mL PBS and the culture was adjusted to a density of 1×10^9 CFU mL⁻¹. Finally, the bacteria suspension was diluted in DMEM, PBS or HBSS to the appropriate MOI.

Preparation of heat-killed L.m.

Heat-killed *L. monocytogenes* (HK L.m.) were prepared by incubating 1 mL of bacteria suspension (1×10^9 CFU) in PBS, at 70° C for 30 min. Efficiency of heat-inactivation of *L. monocytogenes* was tested by plating HK L.m. on blood agar plates before use.

C₁₂FDG labelling of L.m.

L.m. (1×10^9 CFU) were labelled with 350 µg/mL 5-dodecanoylaminofluorescein-di-β-D-galactopyranoside (C₁₂FDG) (ThermoFisher) in 1 mL 0.1 M NaHCO₃, pH 9.6 for 1 h at 37° C. After incubation, L.m. were washed two times with 1 mL cold HBSS. Peritoneal macrophages were infected at a MOI of 10 and then were incubated at 37° C in HBSS with Ca²⁺ and Mg²⁺ in a Tristar2 multimode plate reader LB 942 (Berthold Technologies). Unquenched C₁₂FDG fluorescence was measured at 60 s intervals using standard GFP filters. Inhibition of phagosomal acidification, and thereby acid hydrolases activity, by 100 µM chloroquine served as negative control and completely prevented C₁₂FDG cleavage.

TRITC labelling of L.m.

TRITC-staining solution was prepared by dissolving 5 mg TRITC (Sigma-Aldrich) in 250 µL DMSO. Pellet of L.m. over-night culture was resuspended in 1 mL 5 mM EDTA in PBS. After 5 min centrifugation at 3000 g, 4° C, pellet was resuspended in 990 µL 0.1 M NaHCO₃, pH 9.0. After addition of 10 µL of TRITC-staining solution, L.m. were incubated at RT for 1 h in the dark. Excess of TRITC was removed by 3-5 times washing in 10 mL PBS. Finally, the OD₆₀₀ was determined and the L.m. culture was diluted to the appropriate MOI.

2.2.2 Isolation and purification of macrophages

Isolation of peritoneal cells from infected mice

For isolation of peritoneal macrophages from infected mice, mice were sacrificed by cervical dislocation at 2 h after i.p. infection with 7.5×10^6 L.m. in 0.2 ml PBS. Peritoneal cells were collected by a single peritoneal lavage with 8 mL of ice-cold PBS. For immunofluorescence microscopy, cells were allowed to adhere to sterile glass cover slips for 15 min at 37° C in DMEM supplemented with 10 % FCS.

Purification of peritoneal macrophages

For isolation of peritoneal macrophages from naïve mice, mice were sacrificed by cervical dislocation and the peritoneal cells were isolated by peritoneal lavage using 8 mL ice cold PBS. Afterwards red blood cells were lysed in 5 mL 0.2 % NaCl in H₂O. After 30 seconds isotonic conditions were reconstituted by addition of 5 mL 1.6 % NaCl in H₂O. After red blood cell lysis, cells were prepared for immunomagnetic enrichment. For this, the cells were centrifuged and the cell pellet was resuspended in MACS buffer. Afterward the cells were labeled with CD11b-specific monoclonal antibodies, which are conjugated to paramagnetic beads (CD11b MicroBeads). After 15 minutes of incubation on ice, the cells were separated in accordance with the protocol of the manufacturer (Miltanyi Biotec, Bergisch Gladbach, Germany). Finally, viable cells were counted using Trypan blue exclusion in a Neubauer chamber. Percentage of peritoneal macrophages was determined by FACS analysis. In experiments with CD11^{-/-} mice, both Wt and KO peritoneal cells were used without further enrichment. Similar numbers of F4/80⁺ peritoneal macrophages between Wt and KO samples were verified by FACS analysis.

Preparation of bone marrow-derived macrophages

Mice were sacrificed by cervical dislocation and the skin and muscles were removed from the hind legs. Afterwards, the legs were detached from the mouse and the ends of the femur and shin were opened. The opened bones were rinsed with 5 mL VLE RPMI 1640 medium, using a syringe with a thin needle (0.6 x 30 mm). The released bone marrow was resuspended and collected in a 50 mL falcon tube. After a centrifugation step, the pellet was resuspended in 5 mL NH₄Cl/Tris and incubated for 5 minutes at RT, in order to lyse the red blood cells. Finally, the cells were again centrifuged and the pellet was resuspended in VLE RPMI 1640 medium supplemented with 10 % FCS, 1 % penicillin/streptomycin, 1 % HEPES, 1 % sodium pyruvate and 10 ng/mL recombinant M-CSF. After 7-10 days of incubation at 37° C in CO₂ incubator (5 %), bone marrow cells were differentiated into bone marrow-derived macrophages (BMDM). 24 h prior to infection of BMDM, penicillin/streptomycin was removed.

2.2.3 Flow cytometry analysis of peritoneal cells

Aliquots of 5×10^4 cells in a volume of 50 μ L MACS buffer (either bone marrow-derived macrophages, purified peritoneal macrophages or non-enriched peritoneal exudate cells) were transferred in wells of a 96-well V-bottom plate. After addition of CD16/32 antibody, cells were incubated for 15 minutes on ice in order to block unspecific Fc-binding sites (i. e. Fc γ II and III receptors). Afterwards, cells were incubated with 0.5 μ L fluorescent antibodies from BD Biosciences against F4/80 (clone BM8), CD11b (clone M1/70), Ly6C (clone AL-21) and/or Ly6G (clone 1A8) for 20 min on ice. After incubation, unbound antibodies were removed by three times washing with 150 μ L MACS buffer. Finally, the cells were fixed with 150 μ L FACS Fix and transferred into FACS-tubes. The samples were analyzed via flow cytometry with a FACSCalibur flow cytometer using CellQuest Pro software (BD Biosciences, Heidelberg,

Germany). Cell numbers of F4/80⁺/CD11b⁺ macrophages, Ly6C⁺/Ly6G⁻ inflammatory monocytes and Ly6C⁺/Ly6G⁺ neutrophils were calculated by multiplying the total number of peritoneal cells with the percentage of F4/80⁺/CD11b⁺, Ly6C⁺/Ly6G⁻ or Ly6C⁺/Ly6G⁺ cells, respectively.

2.2.4 Immunofluorescence microscopy

Infection of macrophages

Peritoneal macrophages, bone marrow-derived macrophages or peritoneal exudate cells from infected mice, were allowed to adhere to sterile 13 mm Ø cover glasses at a density of 3 x 10⁵ cells/well in 24-well plates. Non-adherent cells were removed after 1 h by washing once with 1 mL ice-cold PBS. Afterwards, *L. monocytogenes* (either wild-type, LLO-deficient or heat-killed) were added at a MOI of 0.5 or 1 in ice-cold DMEM supplemented with 10 % FCS. Adherence of *L.m.* to the macrophages was synchronized by centrifugation at 850 g, 4° C for 5 min. Non-adherent bacteria were removed by washing three times with 1 mL of ice-cold PBS. Afterwards, pre-warmed DMEM with 10 % FCS was added to the infected cells. At defined time points after infection, the cells were fixed using 3% PFA in PBS for 20 min at RT.

Alternatively, mice were infected intraperitoneally with 7.5 x 10⁶ *L.m.* in 0.2 mL PBS and sacrificed at 2 h p.i.. Peritoneal cells were collected by peritoneal lavage, allowed to adhere to sterile glass cover slips for 15 min at 37° C in DMEM with 10 % FCS and then fixed in 3% PFA in PBS for 20 min at RT.

Staining of cells and bacteria

First, unspecific binding sites were blocked with 1 mL 3 % BSA in PBS for 15 min at RT. Next, extracellular L.m. were stained with primary rabbit anti-*L. monocytogenes* antibody diluted in 3 % BSA blocking buffer for 30 min at RT. After washing three times with PBS, L.m. were stained with secondary goat-anti-rabbit antibody, conjugated to AlexaFluor 405 or 647 fluorescence dye, diluted in 3 % BSA blocking buffer, for 30 min at RT. Afterwards, cells were washed three times with 1 mL PBS. Prior to staining of intracellular L.m., the cells were permeabilized using 0.1 % saponin in PBS for 15 min at RT. Unspecific binding sites were blocked using 3 % BSA and 0.1 % saponin in PBS for 15 min at RT. Intracellular L.m. were stained with primary rabbit anti-*L. monocytogenes* antibody diluted in 3 % BSA and 0.1 % saponin in PBS. After washing with 0.1% saponin in PBS, intracellular L.m. were stained with secondary goat-anti-rabbit antibody, conjugated to AlexaFluor 568 fluorescence dye, diluted in 3 % BSA and 0.1 % saponin in PBS, for 30 min at RT. Cell nucleus (DNA) was stained with DAPI (Sigma-Aldrich), filamentous actin was stained with fluorescent Phalloidin (ThermoFisher). In non-GFP-LC3 transgene macrophages, LC3 was stained with mouse-anti-LC3 antibody (clone 8E10, MBL), overnight at 4° C and secondary goat-anti-mouse antibody, conjugated to AlexaFluor 488 fluorescence dye, diluted in 3 % BSA blocking buffer, for 30 min at RT. Finally, cells were washed three times with PBS and once with H₂O and then mounted on microscope slides in ProLong Gold antifade reagent. Sections of the preparations were analyzed by confocal laser scanning microscopy.

Labelling of lysosomes with fluid phase markers

Peritoneal macrophages adhered to sterile cover glasses at a density of 3×10^5 cells/well in 24-well plate, were pulsed for 1 h with 1.25×10^{11} fluorescent FluoSpheres (Molecular

Probes) with a diameter of 0.02 μm in DMEM + 10 % FCS. Non-endocytosed FluoSpheres were removed by washing three times with 1 mL PBS. Afterwards, fresh DMEM supplemented with 10 % FCS was added and the cells were incubated for 2 h at 37° C, in order to enable the FluoSpheres to accumulate in the lysosomes (chase). Then, the cells were infected and prepared for immunofluorescence microscopy as described above.

2.2.5 Western Blot analysis

Preparation of cell lysates

Purified peritoneal macrophages at a density of 5×10^5 cells/well in 24-well plate or bone marrow-derived macrophages at a density of 7.5×10^5 cells/well in 12-well plate, were allowed to adhere to the bottom of sterile plastic wells. After 1 h of incubation, non-adherent cells were removed by washing with 1 mL of ice-cold PBS. Afterwards, *L. monocytogenes* were added at a MOI of 5 in ice-cold medium. Adherence of L.m. to the macrophages was synchronized by centrifugation at 850 g, 4° C for 5 min. Non-adherent bacteria were removed by washing three times with 1 mL of ice-cold PBS. Uptake of L.m. was initiated by addition of pre-warmed medium to the infected cells. Rapamycin (40 $\mu\text{g mL}^{-1}$ in pre-warmed medium) was used as a positive control for mTOR inactivation and thus p70S6K dephosphorylation. At defined time points (e. g. 120 min post infection or incubation with Rapamycin), cells were washed with ice-cold PBS. Afterwards, PBS was completely removed and cells were lysed with RIPA buffer, which contained protease/phosphatase inhibitors and benzonase, for 10 minutes on a shaker. Alternatively, peritoneal cells from infected mice were isolated by peritoneal lavage, washed in PBS and lysed in 50 μL RIPA buffer. Lysates were transferred into 1.5 mL Eppendorf tubes followed by incubation at 95° C for 5 min. After short condensation on ice, the samples were briefly centrifuged. Protein concentration was determined using BCA Protein Assay Kit in

accordance with the protocol of the supplier (Pierce, Thermo Scientific). Finally, protein concentration was adjusted to 20-30 $\mu\text{g mL}^{-1}$ in 5 x Laemmli buffer and H_2O .

SDS-PAGE and Western Blot

Prior to SDS PAGE, the lysates were incubated at 95° C for 10 min. SDS PAGE was performed in accordance with the protocol of the supplier (Bio-Rad Laboratories, Inc.), using a Criterion Cell filled with (1 x) TGS running buffer and Criterion Cassettes containing a 12 or 16 % Tris/HCl gel for p70S6 kinase or LC3 blot, respectively. After SDS-PAGE, proteins were transferred onto a nitrocellulose membrane in accordance to the protocol of the supplier (Bio-Rad Laboratories, Inc.) using a Trans-Blot Turbo system.

In order to block unspecific binding sites, the membranes were incubated in BSA or milk blocking solution for 30 min at RT. Afterwards, the membranes were incubated with primary antibody in blocking solution overnight at 4° C. Monoclonal antibodies against LC3 and actin (diluted in milk blocking solution) were from Sigma-Aldrich. Monoclonal antibodies against phospho-p40^{phox}, phospho-p70S6K and p70S6K (diluted in BSA blocking solution) were from Cell Signaling. Unbound antibodies were removed by triple washing of the membrane with TBST. Thereafter, membranes were incubated with HRP-conjugated secondary antibodies in blocking solution for 60 min at RT. Again, unbound antibodies were removed by washing two times with TBST and once with TBS. The immune complex was visualized using Amersham ELC Detection reagents (GE Healthcare) or LumiGLO Reserve Chemiluminiscent substrate (KPL Inc.) and detected using the MF-ChemiBIS 3.2 imaging system (DNR Bio Imaging Systems) or Aqfa Curix 60 developing machine with Amersham Hyperfilm ECL (GE Healthcare). PageRuler Prestained Protein Ladder (Thermo Scientific) or High-Range Rainbow Molecular Weight Marker (GE Healthcare) were used for identification of protein size. Specific bands on

immunoblots were quantified by densitometry using ImageJ 1.46h software (Wayne Rasband, NIH, USA).

2.2.6 ASMase activity assay

Peritoneal macrophages infected at a MOI of 1 were lysed in 0.2 % Triton X-100. Protein concentration was determined using BCA Protein Assay Kit in accordance with the protocol of the supplier (Pierce, Thermo Scientific). Breakdown of sphingomyelin into phosphorylcholine and ceramide by ASMase was measured as described before (Wiegmann, Schutze et al. 1994). In brief, 50 µg of protein was incubated for 2 h at 37° C in 250 mM sodium acetate, 1 mM EDTA, pH 5.0 and 0.2 µCi/mL [N-methyl-¹⁴C] sphingomyelin. The amount of radioactive phosphorylcholine produced was quantified by thin layer chromatography.

2.2.7 Transmission electron microscopy

Peritoneal cells from infected mice or peritoneal macrophages infected at a MOI of 1 *in vitro* were fixed in 3% glutaraldehyde and 1% lanthan in 0.1 M cacodylate buffer, pH 7.4 for 10 min at RT and collected as cell pellets after centrifugation. Lanthan served to stain membranes with access to the extracellular milieu to exclude extracellular L.m. from analysis. Cell pellets were postfixed with 1 % osmium tetroxide and 1.5 % K₄Fe(CN)₆ and 0.3 M sucrose in 0.1 M cacodylate buffer and embedded in Epon. Ultrathin sections were cut using an Ultracut E (Reichert Jung). Samples were analyzed after contrasting 10 min with 2 % uranyl acetate followed by 5 min 0.2 % lead citrate using a Zeiss TEM 109 transmission electron microscope at 80 kV.

2.2.8 Analysis of survival of infected mice and bacterial burden

Age- and sex-matched mice were infected intraperitoneally with the LD50 of 5×10^3 L.m. in 0.2 mL PBS and monitored daily for survival. For determination of the bacterial burden, mice were sacrificed at 72 h p.i.. Peritoneal cells were collected by peritoneal lavage, counted and lysed in 0.1 % Triton X-100. Liver and spleen were weighted and homogenized in 0.1 % Triton X-100 with a tissue dissociator gentleMACS in gentleMACS M tubes (Miltenyi Biotech, Bergisch Gladbach, Germany). Serial dilutions were plated on blood agar plates using spiral plater Eddy Jet (IUL, Barcelona, Spain) and CFU/ 10^6 cells or CFU/g organ weight was determined with an automatic colony counter Flash & Go (IUL, Barcelona, Spain).

2.2.9 Quantification of ROS

Peritoneal macrophages were seeded in white, 96-well plate at a density of 5×10^4 cells/well. Cells were infected in ice-cold HBSS at a MOI of 1 or stimulated with 1 ng/mL PMA. After infection or stimulation, peritoneal macrophages were incubated at 37° C in 50 μ M isoluminol (Sigma-Aldrich) and 3.2 U/mL HRP (Merck Millipore) in HBSS with Ca^{2+} and Mg^{2+} . Isoluminol luminescence was measured at 60 s intervals using a Tristar2 multimode plate reader LB 942 (Berthold Technologies).

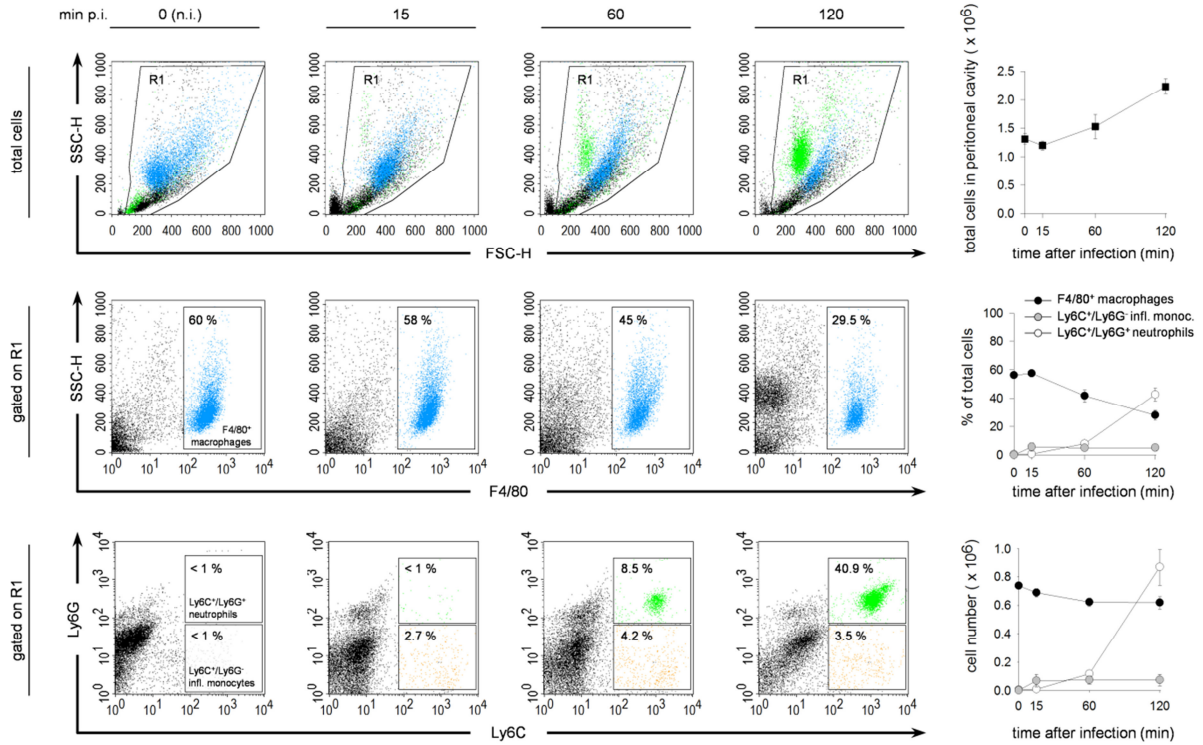
3 Results

3.1 L.m. primarily infects F4/80⁺ macrophages after intraperitoneal injection.

To investigate if L.m. are targeted *in vivo* by canonical autophagy or LAP, we decided to use the model of intraperitoneal infection of mice. The peritoneal cavity harbors a large quantity of immune cells mainly macrophages (Zhang et al. 2008). Additionally, infection of the peritoneal cavity triggers a rapid infiltration of different immune cells such as neutrophils into the peritoneal cavity (Unanue, 1997). For this reason, we wanted to know which cells are primarily infected after intraperitoneal injection of L.m.. Therefore, wild type (Wt) mice were infected intraperitoneally with 7.5×10^6 TRITC-labelled L.m.. At 15, 60 or 120 min post infection (p.i.), peritoneal cells were isolated by peritoneal lavage. The total number of peritoneal cells was quantified and the composition of cells was analyzed by FACS. Non-infected (n.i.) mice contained about 1.4×10^6 cells in the peritoneal cavity. About 60 % of these cells were F4/80⁺ macrophages, whereas Ly6C⁺/Ly6G⁻ inflammatory monocytes and Ly6C⁺/Ly6G⁺ neutrophils were almost absent (Fig. 3 A). At 120 min p.i., the total number of peritoneal cells increased to about 2.2×10^6 cells. At this time point, about 40 % of all peritoneal cells were neutrophils, whereas the percentage of F4/80⁺ macrophages decreased to about 30 %. Nevertheless, the total number of F4/80⁺ macrophages remained more or less unchanged during the 120 min of infection (Fig. 3 A). Interestingly, already 15 min after infection, almost 90 % of macrophages contained TRITC-labelled L.m.. At 120 min after infection, also more than 90 % of macrophages were infected, whereas only 6 % of neutrophils and about 4 % of inflammatory monocytes were positive for TRITC-labelled listeria (Fig. 3 B). These results show that L.m. primarily infects F4/80⁺ macrophages after intraperitoneal injection of L.m.. Therefore, for further analyses we concentrated on peritoneal macrophages.

Figure 3

A



B

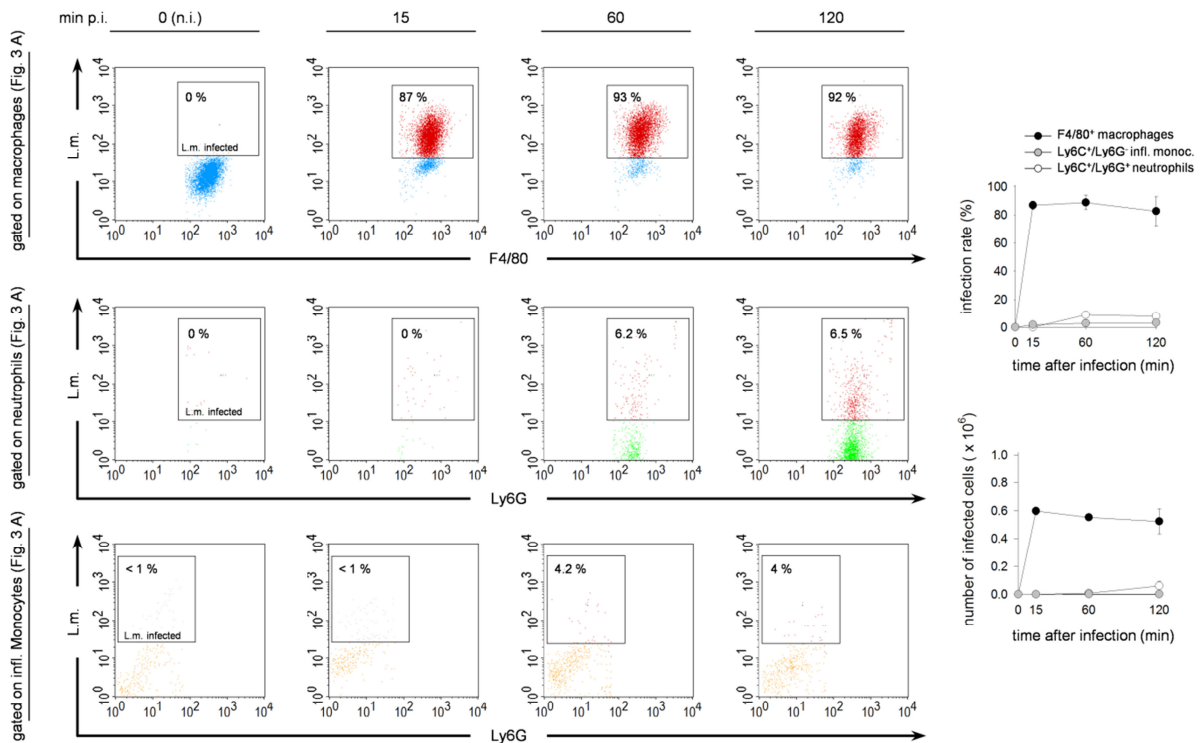


Figure 3: FACS analysis of peritoneal cells from L.m.-infected mice.

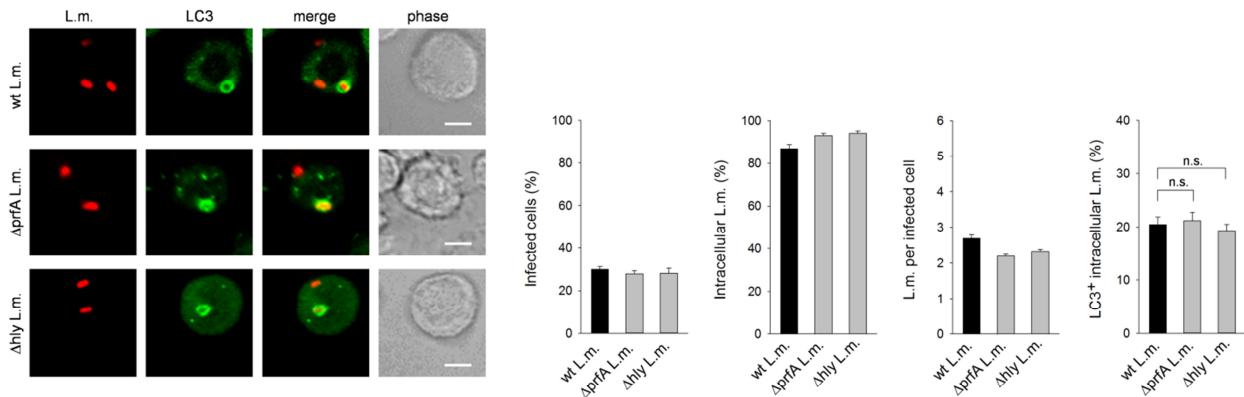
- (A) Wt mice were infected i.p. with 7.5×10^6 TRITC-labelled L.m.. At the indicated time points after infection, peritoneal cells were counted using Trypan Blue exclusion method in a hemocytometer chamber and analyzed by FACS for surface expression of F4/80, Ly6C and Ly6G. Cell numbers of F4/80⁺ macrophages, Ly6C⁺/Ly6G⁻ inflammatory monocytes and Ly6C⁺/Ly6G⁺ neutrophils were calculated by multiplying the total number of peritoneal cells with the percentage of F4/80⁺, Ly6C⁺/Ly6G⁻ or Ly6C⁺/Ly6G⁺ cells, respectively.
- (B) Infection rates of peritoneal cells were determined by analyzing the percentage of TRITC-L.m.-containing cells for each of the individual phagocyte populations. Cells from mice infected with unlabeled L.m. served as a negative control. Non-infected (n.i.) mice were used for t=0 min p.i.. Data are shown as mean +/- SEM from three mice per time point.

3.2 LC3 recruitment to L.m.-containing phagosomes is independent of listerial virulence factors

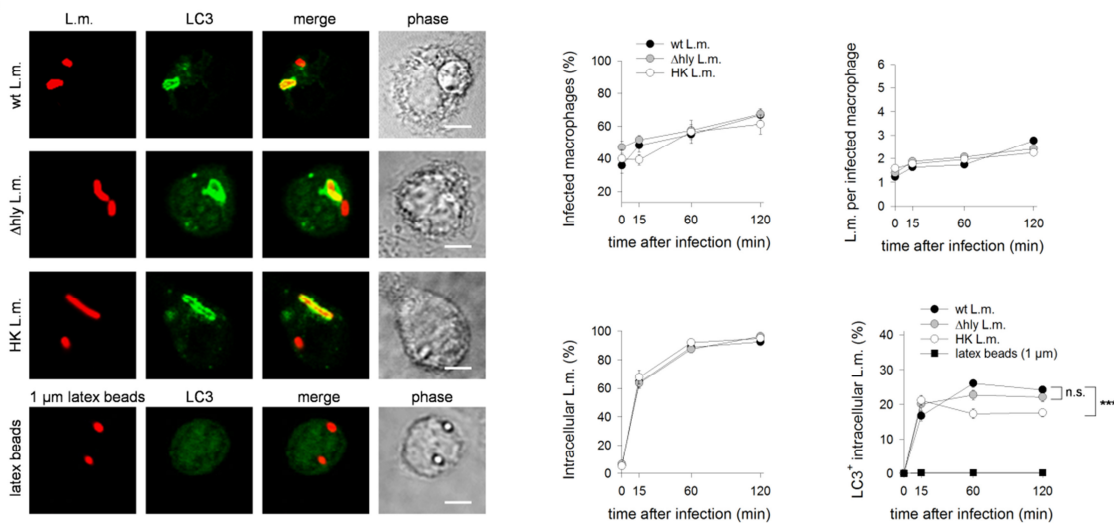
After identification of F4/80⁺ macrophages as primarily infected cell type, we investigated if and how the autophagic marker LC3 is recruited to internalized L.m. in these cells. For this purpose, we infected GFP-LC3 transgenic mice with L.m. and analyzed the co-localization of intracellular listeria with GFP-LC3 in peritoneal macrophages from these mice by fluorescence microscopy. We found that 120 min after infection, about 20 % of intracellular wt L.m. co-localized with LC3. Since it has been reported that listeriolysin O (LLO) is necessary for LC3 recruitment to L.m. in bone marrow-derived macrophages (Lam et al., 2013; Meyer-Morse et al., 2010), we used Δ prfA L.m., which are deficient for the transcriptional master regulator of L.m. virulence factors and Δ hly L.m., which are deficient for the pore-forming toxin LLO, as a negative control for LC3 recruitment. Surprisingly, Δ prfA and Δ hly L.m. co-localized with LC3 to a similar extent as wt L.m. (Fig. 4 A). Noteworthy, infection rate, uptake of L.m. and mean number of L.m. per infected cell were not influenced by listerial virulence factors (Fig. 4 A). Similar data were obtained with peritoneal macrophages infected *in vitro*. Infection rate, uptake of L.m. and mean number of L.m. per infected macrophage were not influenced by listerial virulence factors (Fig. 4 B). LC3 was rapidly recruited to L.m. so that already 15 min after infection, about 20 % of intracellular L.m. co-localized with LC3. Also *in vitro*, infection with Δ hly L.m. triggered LC3 recruitment. Even co-incubation of peritoneal macrophages with heat-killed L.m. (HK L.m.) induced recruitment of LC3 with similar kinetics and to a similar degree as wt L.m.. By contrast, LC3 was not recruited to phagosomes containing 1 μ m latex beads, indicating that LC3 was recruited specifically to bacteria-containing phagosomes (Fig. 4 B).

Figure 4

A



B



C

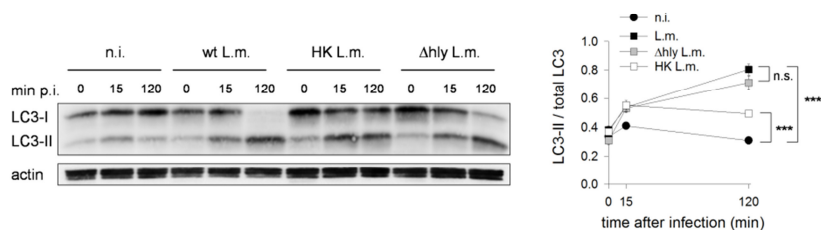


Figure 4: LC3 recruitment to L.m.-containing phagosomes is independent of listerial virulence factors.

- (A) GFP-LC3 transgenic mice were infected i.p. with 7.5×10^6 wt, $\Delta prfA$ or Δhly L.m.. Peritoneal cells were isolated at 2 h p.i.. Peritoneal macrophages were identified morphologically and infection rate, phagocytic uptake of L.m., average number of L.m. per macrophage and percentage of GFP-LC3⁺ intracellular L.m. were quantified by fluorescence microscopy. Representative micrographs are shown. Data are shown as mean \pm SEM of all analyzed cells from three to six individual mice from three independent experiments. Scale bar, 4 μ m.
- (B) Peritoneal macrophages were infected *in vitro* with a MOI of 1 of wt, Δhly or HK L.m., or co-incubated with 1 μ m latex beads. Infection rate, phagocytic uptake of L.m., average number of L.m. per macrophage and co-localization of GFP-LC3 with intracellular L.m. or 1 μ m latex beads were quantified by fluorescence microscopy. Representative micrographs from 2 h p.i. are shown. Data are shown as mean \pm SEM of all analyzed cells from six independent experiments. Scale bar, 4 μ m.
- (C) Peritoneal macrophages were infected *in vitro* with wt, Δhly or HK L.m. at a MOI of 5. Conversion of LC3-I into LC3-II was analyzed by Western blot and quantified by densitometry. Data are shown as mean \pm SEM of five independent experiments. A representative immunoblot is shown. n.s., not significant; * $p < 0.05$, ** $p < 0.01$ and *** $p < 0.001$.

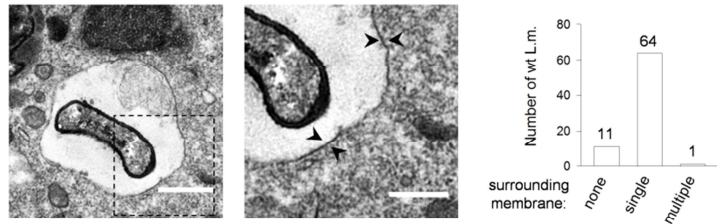
We confirmed the microscopic data by quantifying the LC3 isoforms, i. e. cytosolic LC3-I and membrane-associated (lipidated) LC3-II, by Western blot. In non-infected cells, conversion of cytosolic LC3-I into membrane-associated LC3-II was not observed during a period of 120 min (Fig. 4 C). By contrast, in cells infected with wt L.m., a large proportion of LC3-I was converted into LC3-II indicating strong autophagic activity. Infection with Δ hly L.m. triggered conversion of LC3-I into LC3-II to a similar degree and with similar kinetics as infection with wt L.m.. Remarkably, even co-incubation of peritoneal macrophages with HK L.m. triggered conversion of LC3-I into LC3-II, although to a slightly lower degree than infection with wt L.m. (Fig. 4 C). These data show that, in tissue-resident macrophages, LC3 is recruited to L.m.-containing phagosomes independent of the capability of L.m. to damage the phagosomal membrane or to escape into the cytosol.

3.3 Canonical autophagy is not involved in LC3 recruitment to L.m.-containing phagosomes

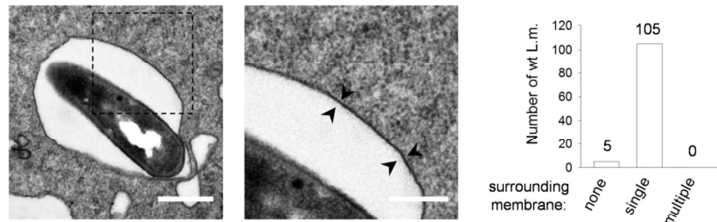
LC3 can be recruited either to cytosolic L.m. by canonical autophagy, resulting in sequestration of L.m. in double-membrane autophagosomes (Rich et al., 2003), or to L.m. in single-membrane vesicles by LC3-associated phagocytosis (LAP) (Lam et al., 2013). To investigate by which of these two alternative pathways L.m. are targeted *in vivo*, we analyzed the membrane-ultrastructure of listeria-containing compartments in macrophages from infected mice by transmission electron microscopy. At 2 h p.i., more than 80 % of intracellular L.m. were surrounded by a single membrane. By contrast, less than 1 % of L.m. were surrounded by multiple membranes. About 15 % of L.m. had escaped from the phagosomes to become cytosolic (Fig. 5 A). In macrophages infected *in vitro*, more than 95 % of intracellular L.m. were surrounded by a single membrane. Less than 5 % of L.m. escaped into the cytoplasm and L.m. surrounded by double- or multiple membranes were not present (Fig. 5 B).

Figure 5

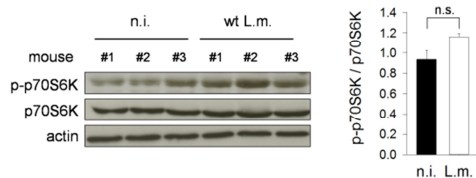
A



B



C



D

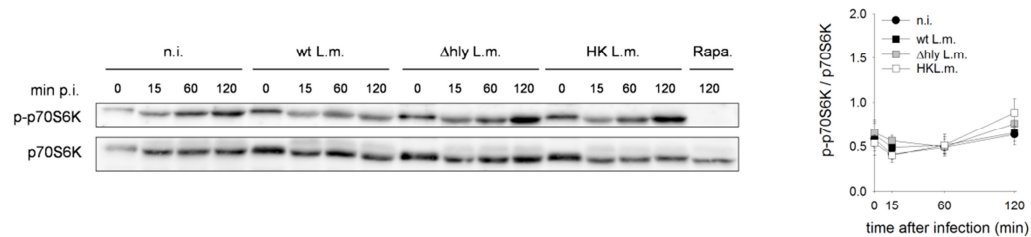


Figure 5: Canonical autophagy is not involved in LC3 recruitment to L.m.-containing phagosomes.

- (A) Peritoneal cells were isolated at 2 h after i.p. infection of mice with 7.5×10^6 wt L.m.. Membrane structures surrounding L.m. were analyzed by transmission electron microscopy. A representative micrograph is shown. Right micrograph is a magnification of the inset indicated by the black box. Arrow heads indicate single membrane. Scale bars, 500 nm and 250 nm (insert).
- (B) Peritoneal macrophages were infected *in vitro* with wt L.m. at a MOI of 1. Membrane structures surrounding L.m. at 1 h p.i. were analyzed by transmission electron microscopy. A representative micrograph is shown. Right micrograph is a magnification of the inset indicated by the black box. Arrow heads indicate single membrane. Scale bars, 500 nm and 250 nm (insert).
- (C) Peritoneal cells were isolated from naïve mice or at 2 h after i.p. infection with 7.5×10^6 wt L.m.. Phosphorylation status of p70S6K in non-infected mice and after L.m. infection was analyzed by Western blot and quantified by densitometry. A representative immunoblot is shown. Each lane represents an individual mouse. Data are shown as mean \pm SEM of six individual mice from two independent experiments.
- (D) Phosphorylation status of p70S6K after infection *in vitro* with wt, Δ hly or HK L.m. at a MOI of 5 was analyzed by Western blot. 40 μ g/ml rapamycin was used as a positive control for mTOR inactivation and thus p70S6K dephosphorylation. P70S6K phosphorylation was quantified by densitometry. Data are shown as mean \pm SEM of five independent experiments. A representative immunoblot is shown.

Next to the presence of multiple or single membranes, the status of the mTOR pathway allows to dissect canonical autophagy from non-canonical autophagy such as LAP. Initiation of canonical autophagy, but not that of LAP, requires inactivation of mTOR (Mehta et al., 2014) that results in dephosphorylation of the mTOR substrate p70S6K (Klionsky et al., 2016). In macrophages from L.m.-infected mice, p70S6K remained phosphorylated to a similar degree as in macrophages from non-infected mice (Fig. 5 C). *In vitro*, incubation of macrophages with rapamycin induced a complete dephosphorylation of p70S6K, whereas p70S6K remained phosphorylated in macrophages infected with wt, Δ hly or HK L.m. (Fig. 5 D). These data indicate that LC3 is recruited to L.m.-containing phagosomes not by canonical autophagy, but by LC3-associated phagocytosis.

3.4 LC3 is recruited to L.m.-containing phagosomes by LC3-associated phagocytosis.

In order to prove that canonical autophagy is not involved in LC3 recruitment to L.m.-containing phagosomes, we used mice with a myeloid cell-specific knockout of FIP200 (FIP200^{MYEL-KO}), which is part of the Ulk complex. While initiation of canonical autophagy essentially depends on Ulk complex activation, independence from Ulk complex components is one of the hallmarks of LAP (Martinez et al., 2015). First, we verified that expression of FIP200 in macrophages from FIP200^{MYEL-KO} mice is almost completely abrogated (Fig. 6 A). Next, we confirmed that these cells are unable to activate canonical autophagy. While starvation induced conversion of LC3-I into LC3-II in Wt macrophages, indicating ongoing canonical autophagy, conversion of LC3-I into LC3-II was abrogated in FIP200^{MYEL-KO} macrophages (Fig. 6 B). Furthermore, stimulation with the mTOR inhibitor rapamycin did not induce canonical autophagy in macrophages from FIP200^{MYEL-KO} mice. Yet, importantly, L.m. infection still induced LC3 conversion in these cells (Fig. 6 C).

Figure 6

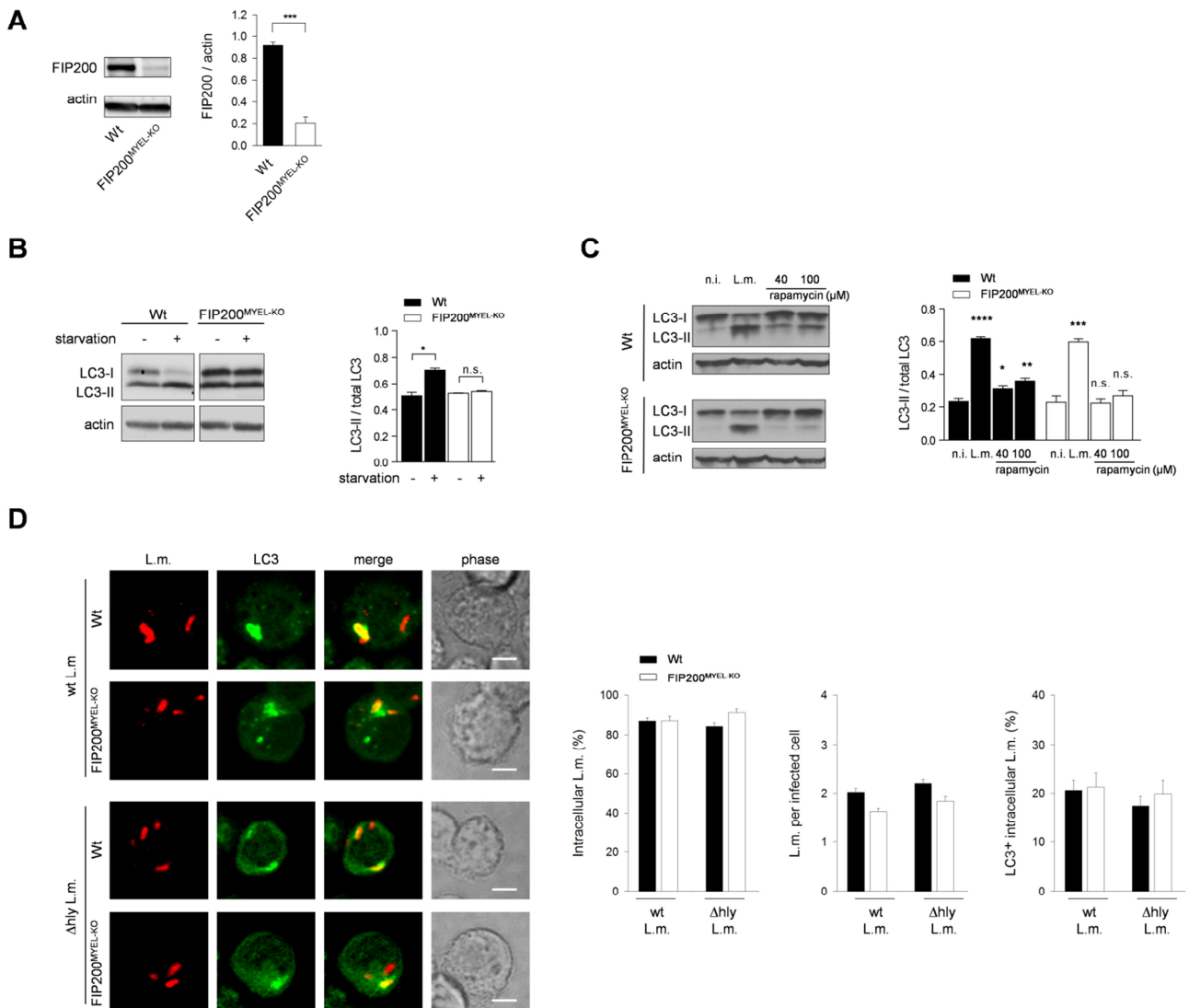


Figure 6: LC3 is recruited to L.m.-containing phagosomes by LC3-associated phagocytosis.

- (A) Expression of FIP200 in macrophages of Wt and FIP200^{MYEL-KO} mice was analyzed by Western blot and quantified by densitometry. Data are shown as mean \pm SEM of three independent experiments. A representative immunoblot is shown.
- (B) Conversion of LC3-I into LC3-II in macrophages of Wt and FIP200^{MYEL-KO} mice starved for 1 h in HBSS was analyzed by Western blot and quantified by densitometry. Data are shown as mean \pm SEM of three independent experiments. Representative immunoblots are shown.
- (C) Conversion of LC3-I into LC3-II in macrophages of Wt and FIP200^{MYEL-KO} mice infected with L.m. at a MOI of 5, or stimulated with 40 or 100 μ g/ml rapamycin for 1 h, was analyzed by Western blot and quantified by densitometry. Data are shown as mean \pm SEM of three independent experiments. Representative immunoblots are shown.
- (D) Peritoneal cells from GFP-LC3 transgenic Wt and FIP200^{MYEL-KO} mice were isolated at 2 h after i.p. infection with 7.5×10^6 wt or Δ hly L.m.. Phagocytic uptake of L.m., the average number of L.m. per infected macrophage and percentage of GFP-LC3⁺ intracellular L.m. were quantified by fluorescence microscopy. Representative micrographs are shown. Data are shown as mean \pm SEM of all analyzed cells from three individual mice from three independent experiments. Scale bar, 4 μ m.
n.s., not significant; * $p < 0.05$, ** $p < 0.01$ and *** $p < 0.001$.

In addition, wt as well as Δ hly L.m. co-localized with LC3 in macrophages from infected FIP200^{MYEL-KO} mice (Fig. 6 D). This finding that LC3 is recruited to L.m.-containing phagosomes

even in macrophages deficient for canonical autophagy and independently of the Ulk complex, strongly indicated ongoing LAP.

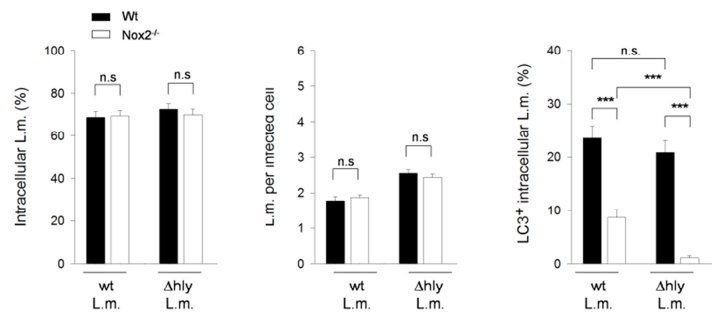
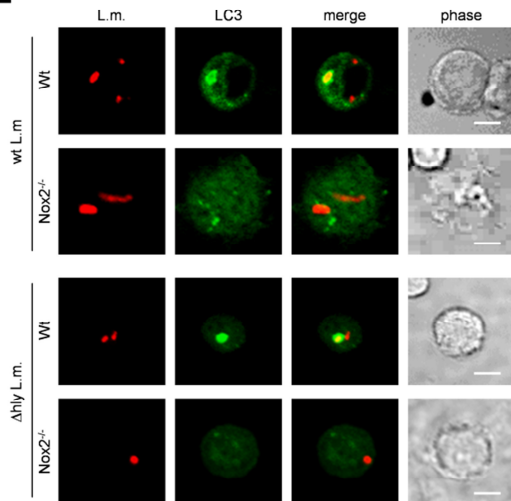
Another hallmark of LAP is the requirement of ROS production by the NADPH oxidase Nox2 (Huang et al., 2009; Lam et al., 2013). In order to confirm that LC3 is recruited to L.m.-containing phagosomes by LAP, we infected GFP-LC3 transgenic Wt and Nox2^{-/-} mice with wt and Δ hly L.m. and analyzed the co-localization of intracellular L.m. with GFP-LC3. Co-localization of L.m. with LC3 was significantly reduced in macrophages from infected Nox2^{-/-} mice, whereas uptake and mean number of L.m. per cell were not altered (Fig. 6 E). Also after infection of macrophages *in vitro*, co-localization of L.m. with LC3 in Nox2^{-/-} macrophages was strongly reduced, which was even more pronounced in the case of Δ hly and HK L.m. (Fig. 6 F).

We next tested if other sources of ROS but Nox2 contribute to LC3 recruitment to L.m.-containing phagosomes. For this purpose, we analyzed co-localization of L.m. with LC3 in Nox1- and Nox4-deficient macrophages. However, co-localization of wt L.m. with LC3 was unaltered in peritoneal macrophages from Nox1^{-/-} or Nox4^{-/-} mice (Fig. 6 G). Inhibition of mitochondrial ROS production with rotenone did also not influence co-localization of L.m. with LC3. General scavenging of ROS with N-acetyl cysteine (NAC) did not reduce co-localization of L.m. with LC3 below the level observed in Nox2^{-/-} macrophages (Fig. 6 G). Furthermore, in contrast to wt macrophages, Nox2^{-/-} macrophages do not produce detectable amounts of ROS after infection with wt, Δ hly or HK L.m. or pharmacological stimulation with PMA (Gluschko and Herb et al., 2018) indicating Nox2 as the source of the ROS produced by L.m.-infected macrophages. Together, these data show that exclusively ROS produced by Nox2 are required to induce recruitment of LC3 to L.m.-containing phagosomes.

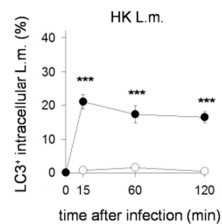
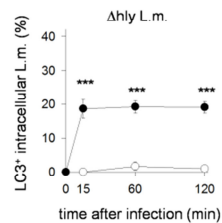
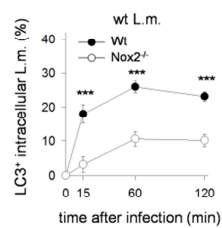
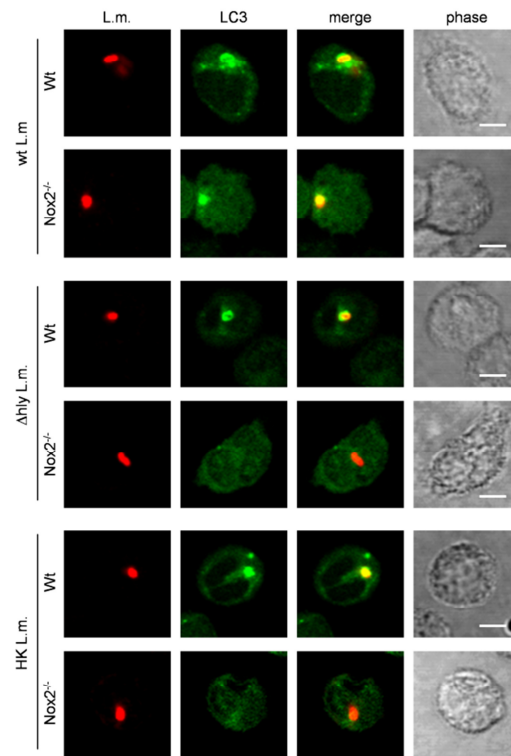
Collectively, due to the findings that L.m. were found exclusively in single-membrane vesicles and that LC3 recruitment was completely independent of mTOR and FIP200 but required ROS production by Nox2, we concluded that LC3 targeting of L.m. *in vivo* was exclusively by LAP and not by canonical autophagy.

Figure 6 (continued)

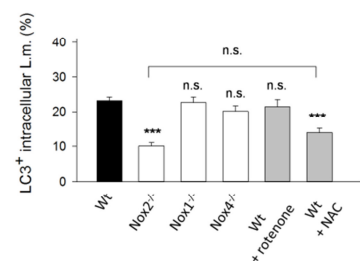
E



F



G

**Figure 6 (continued): LC3 is recruited to L.m.-containing phagosomes by LC3-associated phagocytosis.**

- (E) Peritoneal cells from GFP-LC3 transgenic Wt and Nox2^{-/-} mice were isolated at 2 h after i.p. infection with 7.5×10^6 wt or Δhly L.m.. Phagocytic uptake of L.m., the average number of L.m. per macrophage and percentage of GFP-LC3⁺ intracellular L.m. were quantified by fluorescence microscopy. Representative micrographs are shown. Data are shown as mean \pm SEM of all analyzed cells from three individual mice from three independent experiments. Scale bar, 4 μ m.
- (F) Peritoneal macrophages from Wt and Nox2^{-/-} mice were infected *in vitro* with wt, Δhly or HK L.m. at a MOI of 1. Co-localization of GFP-LC3 with intracellular L.m. was quantified by fluorescence microscopy. Representative micrographs from 2 h p.i. are shown. Data are shown as mean \pm SEM of all analyzed cells from three independent experiments. Scale bar, 4 μ m.
- (G) Peritoneal macrophages from Wt, Nox2^{-/-}, Nox1^{-/-} and Nox4^{-/-} macrophages were infected *in vitro* with wt L.m. at a MOI of 1. Where indicated, macrophages were infected in the presence of 100 μ M rotenone or 50 mM N-acetyl cysteine. Co-localization of GFP-LC3 with intracellular L.m. was quantified by fluorescence microscopy. Data are shown as mean \pm SEM of all analyzed cells from three independent experiments. Statistical significance compared to the corresponding Wt sample was determined. n.s., not significant; * $p < 0.05$, ** $p < 0.01$ and *** $p < 0.001$.

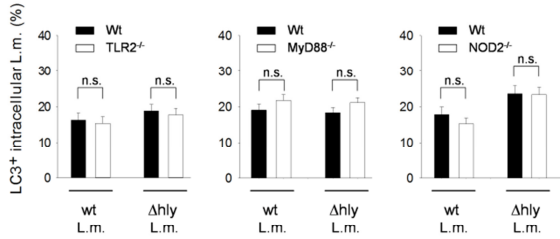
3.5 Mac-1 is the pattern recognition receptor inducing ROS production by Nox2 and LAP in L.m.-infected macrophages.

Because of the essentiality of Nox2 for the initiation of LAP, we next addressed the question about the mechanisms of Nox2 activation in L.m.-infected macrophages. We have shown that, in macrophages from TLR2^{-/-}, MyD88^{-/-} and NOD2^{-/-} mice, ROS production after infection with wt, Δ hly or HK L.m. is unaltered (Gluschko and Herb et al., 2018). Moreover, co-localization of wt and Δ hly L.m. with LC3 in macrophages from infected TLR2^{-/-}, MyD88^{-/-} and NOD2^{-/-} mice was also unaltered (Fig. 7 A). Also after infection of macrophages *in vitro*, co-localization of wt, Δ hly or HK L.m. with LC3 in TLR2^{-/-}, MyD88^{-/-} and NOD2^{-/-} macrophages was indistinguishable from that in Wt macrophages (Fig. 7 B). These data indicate that neither TLRs nor NOD2 are required for Nox2 activation and induction of LAP in response to L.m. infection.

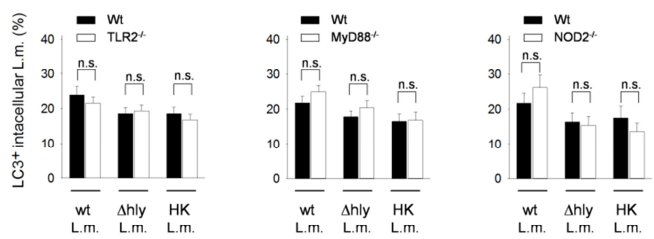
In search for the host cell receptor initiating L.m.-induced Nox2 and LAP activation, we next focused on the β_2 integrin Mac-1. Peritoneal macrophages from mice deficient for the CD11b subunit of Mac-1 (CD11b^{-/-}) produce significantly less ROS after infection with wt or HK L.m., while ROS production after stimulation with PMA is normal (Gluschko and Herb et al., 2018). Moreover, LC3 recruitment to L.m.-containing phagosomes in macrophages from CD11b-deficient mice was significantly reduced (Fig. 7 C). Similarly, *in vitro* infection of CD11b^{-/-} macrophages resulted in reduced recruitment of LC3 to phagosomes containing wt, Δ hly or HK L.m.. The phagocytic uptake of L.m. by CD11b^{-/-} macrophages was not reduced yet slightly delayed (Fig. 7 D). These data demonstrate that interaction of L.m. with Mac-1 is required for initiation of LAP.

Figure 7

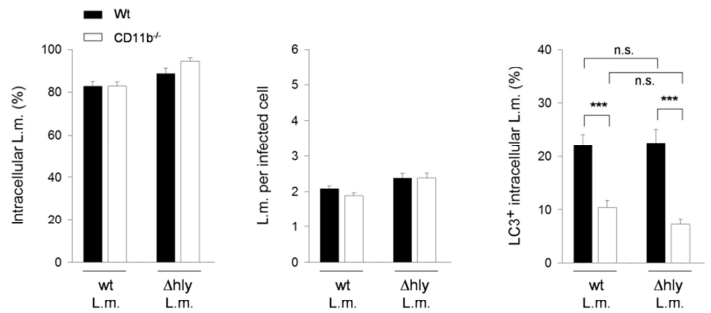
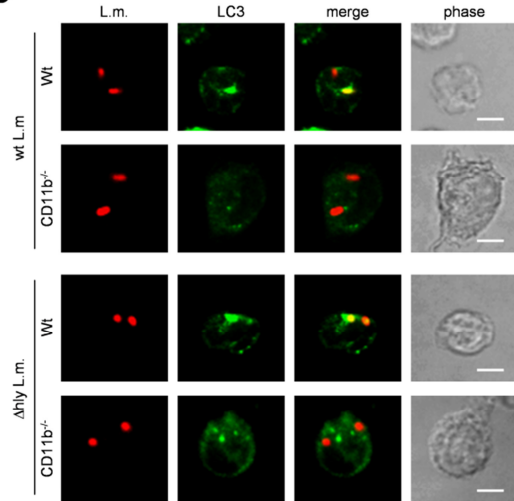
A



B



C



D

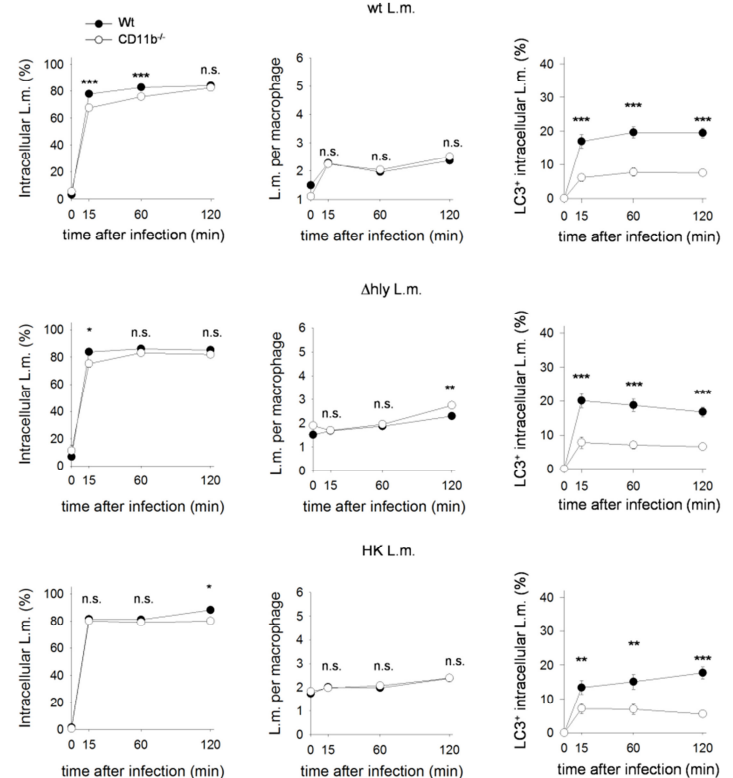
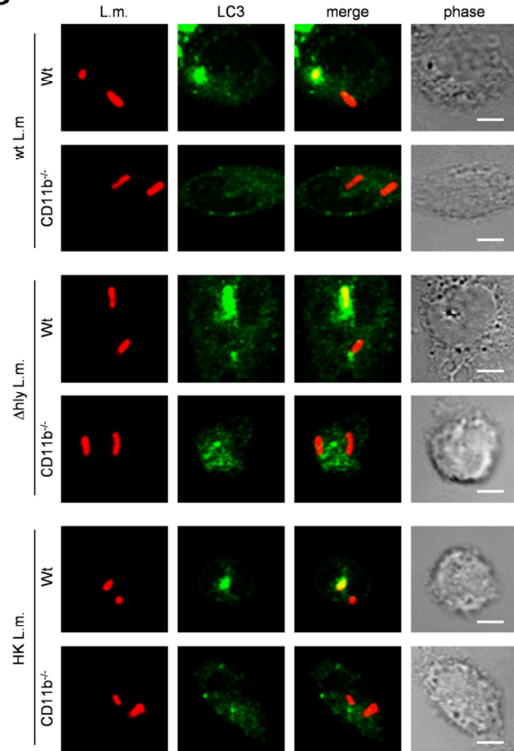


Figure 7: Mac-1 is the pattern recognition receptor inducing ROS production by Nox2 and LAP in L.m.-infected macrophages.

(A) GFP-LC3 transgenic Wt, TLR2^{-/-}, MyD88^{-/-} or NOD2^{-/-} mice were infected i.p. with 7.5 x 10⁶ wt or Δhly L.m.. At 2 h p.i., GFP-LC3⁺ intracellular L.m. in peritoneal cells were quantified by fluorescence microscopy. Data are shown as mean +/- SEM of all analyzed cells from three individual mice from three independent experiments.

(continued on next page)

Figure 7 continued...

- (B) Peritoneal macrophages from GFP-LC3 transgenic Wt, TLR2^{-/-}, MyD88^{-/-} or NOD2^{-/-} mice were infected *in vitro* with wt, Δ hly or HK L.m. at a MOI of 1. GFP-LC3⁺ intracellular L.m. at 2 h p.i. were quantified by fluorescence microscopy. Data are shown as mean \pm SEM of all analyzed cells from three independent experiments.
- (C) Peritoneal cells from GFP-LC3 transgenic Wt and CD11b^{-/-} mice were isolated at 2 h after i.p. infection with 7.5 x 10⁶ wt or Δ hly L.m.. Phagocytic uptake of L.m., the average number of L.m. per macrophage and percentage of GFP-LC3⁺ intracellular L.m. were quantified by fluorescence microscopy. Representative micrographs are shown. Data are shown as mean \pm SEM of all analyzed cells from three individual mice from three independent experiments. Scale bar, 4 μ m.
- (D) Peritoneal macrophages from Wt and CD11b^{-/-} mice were infected *in vitro* with wt, Δ hly or HK L.m. at a MOI of 1. Phagocytic uptake of L.m., the average number of L.m. per macrophage and percentage of GFP-LC3⁺ intracellular L.m. were quantified by fluorescence microscopy. Representative micrographs from 2 h p.i. are shown. Data are shown as mean \pm SEM of all analyzed cells from three independent experiments. Scale bar, 4 μ m. n.s., not significant; * p < 0.05, ** p < 0.01 and *** p < 0.001

3.6 Mac-1 induces ROS production by Nox2 and LAP through activation of acid sphingomyelinase

Activation of Nox2 has been shown to require relocation into ceramide-enriched membrane platforms generated by acid sphingomyelinase (ASMase) (Zhang et al., 2008). Therefore, we investigated if Mac-1 regulates ROS production by Nox2 and LAP by activating ASMase. Indeed, ASMase activity after L.m. infection was significantly reduced in CD11b^{-/-} macrophages (Fig. 8 A) suggesting ASMase as a downstream target of Mac-1. Furthermore, the phosphorylated form of the regulatory Nox2 subunit p40^{phox} failed to appear in L.m.-infected ASMase^{-/-} macrophages (Fig. 8 B), which is yet required for Nox2 activation (Chessa et al., 2010). Furthermore, ASMase^{-/-} macrophages produced markedly reduced amounts of ROS after infection with wt, Δ hly or HK L.m. but not after stimulation with PMA (Fig. 8 C). These data indicate that activation of ASMase by Mac-1 is required for Nox2 activation in L.m.-infected macrophages. Accordingly, ASMase deficiency phenocopied Nox2 deficiency in that recruitment of LC3 to L.m.-containing phagosomes was significantly reduced when ASMase^{-/-} macrophages were infected with L.m. and almost completely abrogated when challenged with Δ hly or HK L.m.. Phagocytic uptake of L.m. by ASMase^{-/-} macrophages was unimpaired (Fig. 8 D).

Figure 8

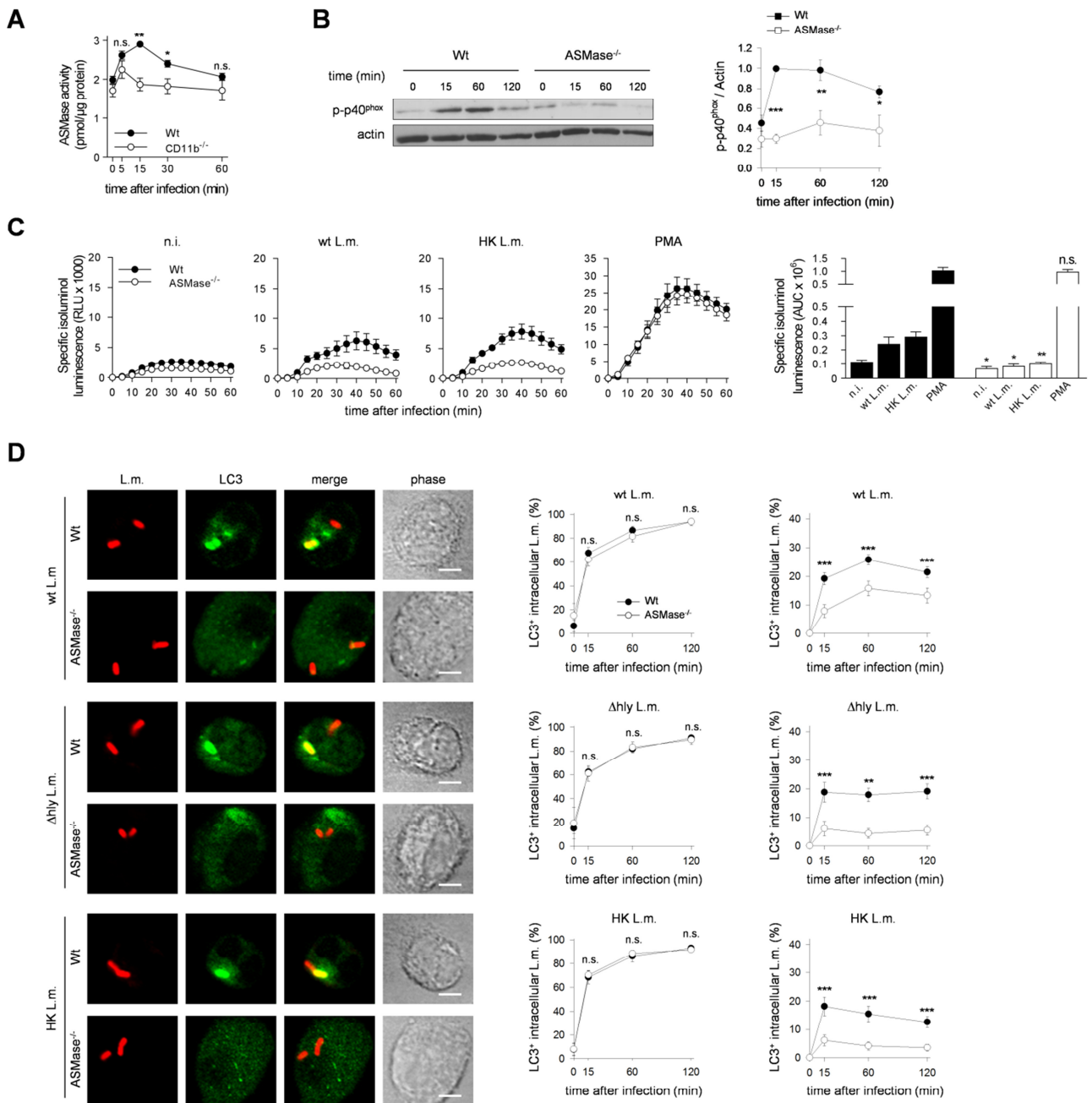


Figure 8: Mac-1 induces ROS production by Nox2 and LAP through activation of acid sphingomyelinase.

- (A) Peritoneal cells from Wt and CD11b^{-/-} mice were infected *in vitro* with wt L.m. at a MOI of 1 and breakdown of sphingomyelin into phosphorylcholine and ceramide by ASMase was analyzed. Data are shown as mean \pm SEM of three independent experiments.
- (B) Phosphorylation status of p40^{phox} in Wt and ASMase^{-/-} peritoneal macrophages after *in vitro* infection with L.m. at a MOI of 5 was analyzed by Western blot and quantified by densitometry. A representative immunoblot is shown. Data are shown as mean \pm SEM of four independent experiments.
- (C) ROS production by Wt and ASMase^{-/-} peritoneal macrophages after *in vitro* infection with wt or HK L.m. at a MOI of 1 or stimulation with PMA was measured using isoluminol. The kinetics of ROS production and the area under the curve (AUC) as a measure for the total amount of ROS produced are shown. Data are shown as mean \pm SEM of three independent experiments and statistical significance compared to the corresponding Wt sample was determined.
- (D) Peritoneal macrophages from GFP-LC3 transgenic Wt and ASMase^{-/-} mice were infected *in vitro* with wt, Δ hly or HK L.m. at a MOI of 1. Uptake and percentage of GFP-LC3⁺ intracellular L.m. were quantified by fluorescence microscopy. Representative micrographs from 2 h p.i. are shown. Data are shown as mean \pm SEM of all analyzed cells from five independent experiments. Scale bar, 4 μ m.
n.s., not significant; * $p < 0.05$, ** $p < 0.01$ and *** $p < 0.001$.

Collectively, these data show that interaction of L.m. with Mac-1 is important for activation of ASMase, which is a prerequisite for Nox2 activation and subsequent LC3 recruitment by LAP.

3.7 LAP increases fusion of L.m.-containing phagosomes with lysosomes

ASMase regulates fusion of L.m.-containing phagosomes with lysosomes, which is critical for immunity to L.m. (Schramm et al., 2008; Utermohlen et al., 2003). We therefore addressed the question if LAP, being downstream of ASMase, promotes fusion of L.m.-containing phagosomes with lysosomes resulting in increased degradative capacity. To visualize the transfer of lysosomal cargo, such as lysosomal acid hydrolases and other degradative enzymes, during phago-lysosomal fusion, we pre-loaded lysosomes with fluorescent latex beads of a diameter of 20 nm. Interestingly, L.m. in LC3-positive (LC3⁺) phagosomes co-localized significantly more often with the lysosomal latex beads than L.m. in LC3-negative (LC3⁻) phagosomes (Fig. 9 A). Similar data were obtained for phagosomes containing Δ hly or HK L.m. showing a strong correlation between presence of LC3 and acquisition of lysosomal cargo (Fig. 9 A).

To investigate if LAP promotes phago-lysosomal fusion or if LC3 is rather recruited to already fused phago-lysosomes, we used mice with a myeloid cell-specific deficiency for Atg7 ($Atg7^{MYEL-KO}$). Atg7 is involved in the conjugation of LC3 to the membranes of phagosomes and is therefore essential for LAP (Martinez et al., 2015). First, we verified that expression of Atg7 in macrophages from $Atg7^{MYEL-KO}$ mice is almost completely abrogated (Fig. 9 B). Next, we analyzed whether these cells failed to recruit LC3 to L.m.-containing phagosomes. Indeed, in $Atg7^{MYEL-KO}$ macrophages, wt as well as Δ hly L.m. did neither co-localize with LC3 (Fig. 9 C) nor induce LC3 conversion (Fig. 9 D), indicating defective LAP.

Figure 9

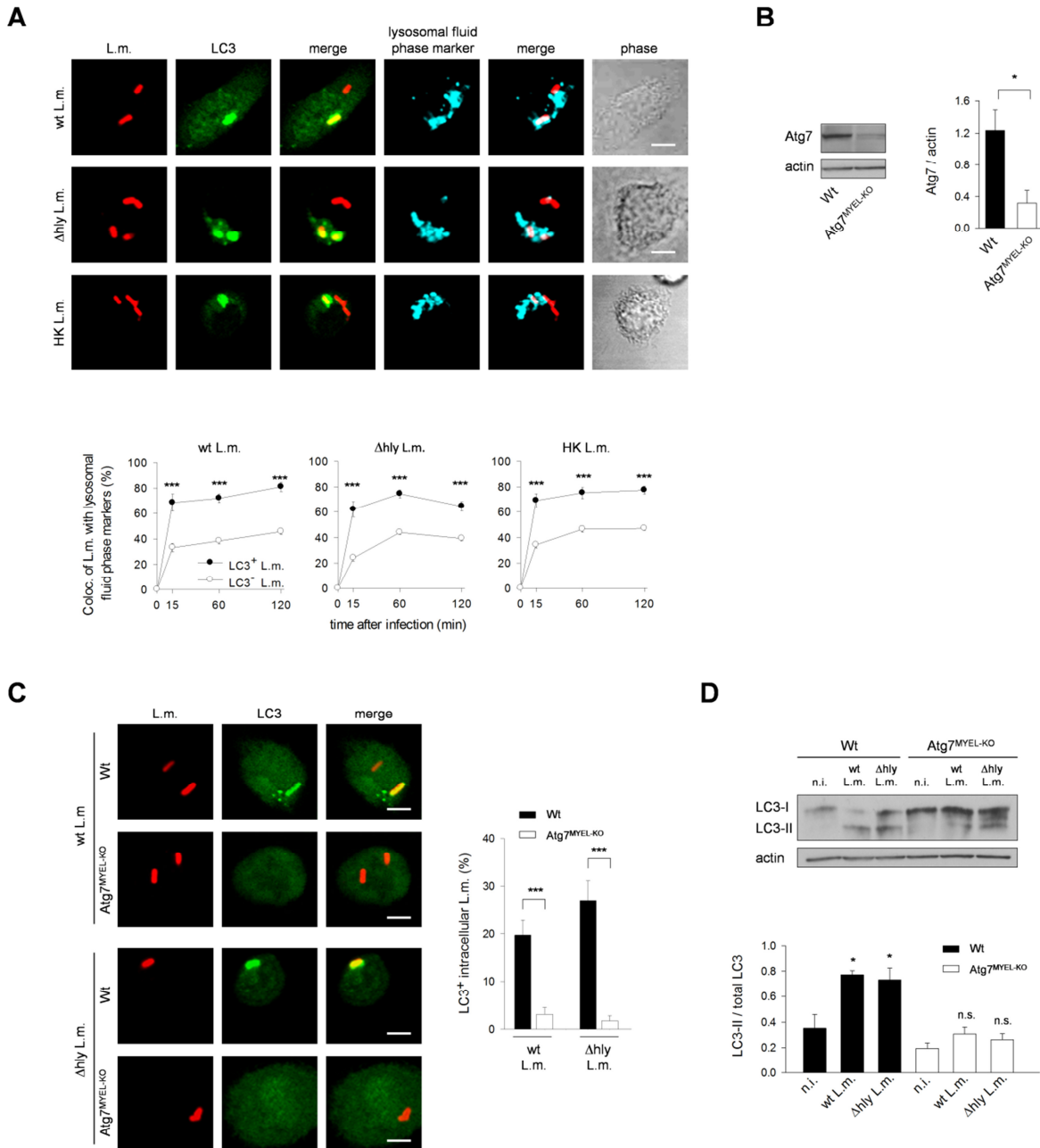


Figure 9: LAP increases fusion of L.m.-containing phagosomes with lysosomes.

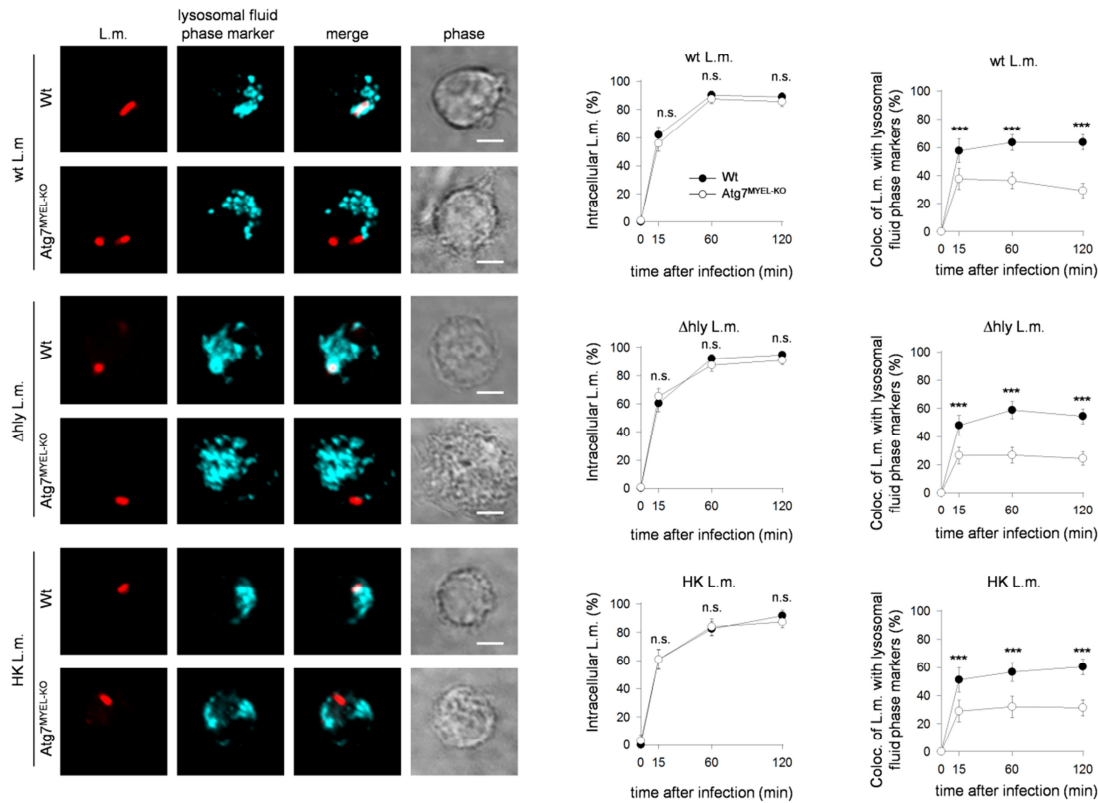
- (A) Lysosomes of peritoneal macrophages from GFP-LC3 transgenic mice were pulse-chase labelled with 20 nm latex beads and then infected *in vitro* with wt, Δ hly or HK L.m. at a MOI of 1. Transfer of lysosomal latex beads into L.m.-containing phagosomes was analyzed by fluorescence microscopy. Representative micrographs from 2 h p.i. are shown. Data are shown as mean \pm SEM of all analyzed cells from three independent experiments. Scale bar, 4 μ m.
- (B) Expression of Atg7 in Wt and Atg7^{MYEL-KO} peritoneal macrophages was analyzed by Western blot and quantified by densitometry. Data are shown as mean \pm SEM of two independent experiments. A representative immunoblot is shown.
- (C) Peritoneal macrophages from Wt and Atg7^{-/-} mice were infected *in vitro* with wt or Δ hly L.m. at a MOI of 1. GFP-LC3⁺ intracellular L.m. at 2 h p.i. were quantified by fluorescence microscopy. Representative micrographs are shown. Data are shown as mean \pm SEM of all analyzed cells. Scale bar, 4 μ m.
- (D) Peritoneal macrophages from Wt and Atg7^{-/-} mice were infected *in vitro* with wt or Δ hly L.m. at a MOI of 5. Conversion of LC3-I into LC3-II at 2 h p.i. was analyzed by Western blot and quantified by densitometry. Data are shown as mean \pm SEM of three independent experiments. A representative immunoblot is shown. n.s., not significant; * $p < 0.05$, ** $p < 0.01$ and *** $p < 0.001$.

Thereafter, we infected Atg7-deficient macrophages with wt, Δ hly and HK L.m. and analyzed co-localization of L.m. with lysosomal fluid phase markers. As shown in Figure 9 E, co-localization of L.m. with lysosomal cargo was significantly reduced in Atg7^{MYEL-KO} macrophages, while phagocytic uptake of L.m. was not altered. Similar data were obtained with Δ hly and HK L.m., excluding listerial virulence factors as cause of reduced acquisition of lysosomal cargo in Atg7-deficient macrophages. Thus, incapability of Atg7-deficient macrophages to recruit LC3 to L.m.-containing phagosomes significantly impaired acquisition of lysosomal cargo indicating that LAP promotes fusion of L.m.-containing phagosomes with lysosomes.

In addition, we wanted to directly analyze the enzymatic activity of lysosomal enzymes in Atg7-deficient macrophages after L.m. infection. In order to functionally assess if LAP increases exposure of L.m. to lysosomal acid hydrolases, we labelled L.m. with 5-dodecanoylaminofluorescein-di- β -D-galactopyranoside (C₁₂FDG) that becomes fluorescent upon cleavage by the lysosomal acid hydrolase β -galactosidase. We infected Atg7^{MYEL-KO} macrophages with C₁₂FDG-labelled L.m. and measured the fluorescence signal, which represents β -galactosidase activity. In Atg7^{MYEL-KO} macrophages infected with wt, Δ hly or HK L.m., C₁₂FDG fluorescence was significantly reduced indicating reduced exposure of L.m. to β -galactosidase (Figure 9 F). Together, these data indicate that LAP increases exposure of L.m. to lysosomal acid hydrolases by promoting fusion of L.m.-containing phagosomes with lysosomes.

Figure 9 (continued)

E



F

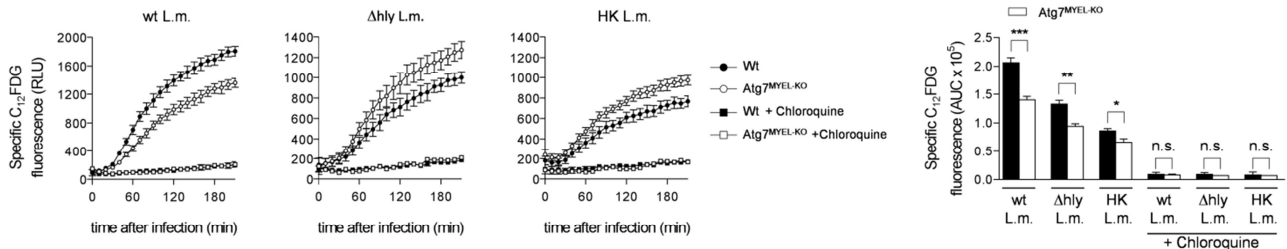


Figure 9 (continued): LAP increases fusion of L.m.-containing phagosomes with lysosomes.

(E) Lysosomes of peritoneal macrophages from Wt or Atg7^{MYEL-KO} mice were pulse-chase labelled with 20 nm latex beads and then infected *in vitro* with wt, Δ hly or HK L.m. at a MOI of 1. Uptake of L.m. and transfer of lysosomal latex beads into L.m.-containing phagosomes was analyzed by fluorescence microscopy. Representative micrographs from 2 h p.i. are shown. Data are shown as mean \pm SEM of all analyzed cells from three independent experiments. Scale bar, 4 μ m.

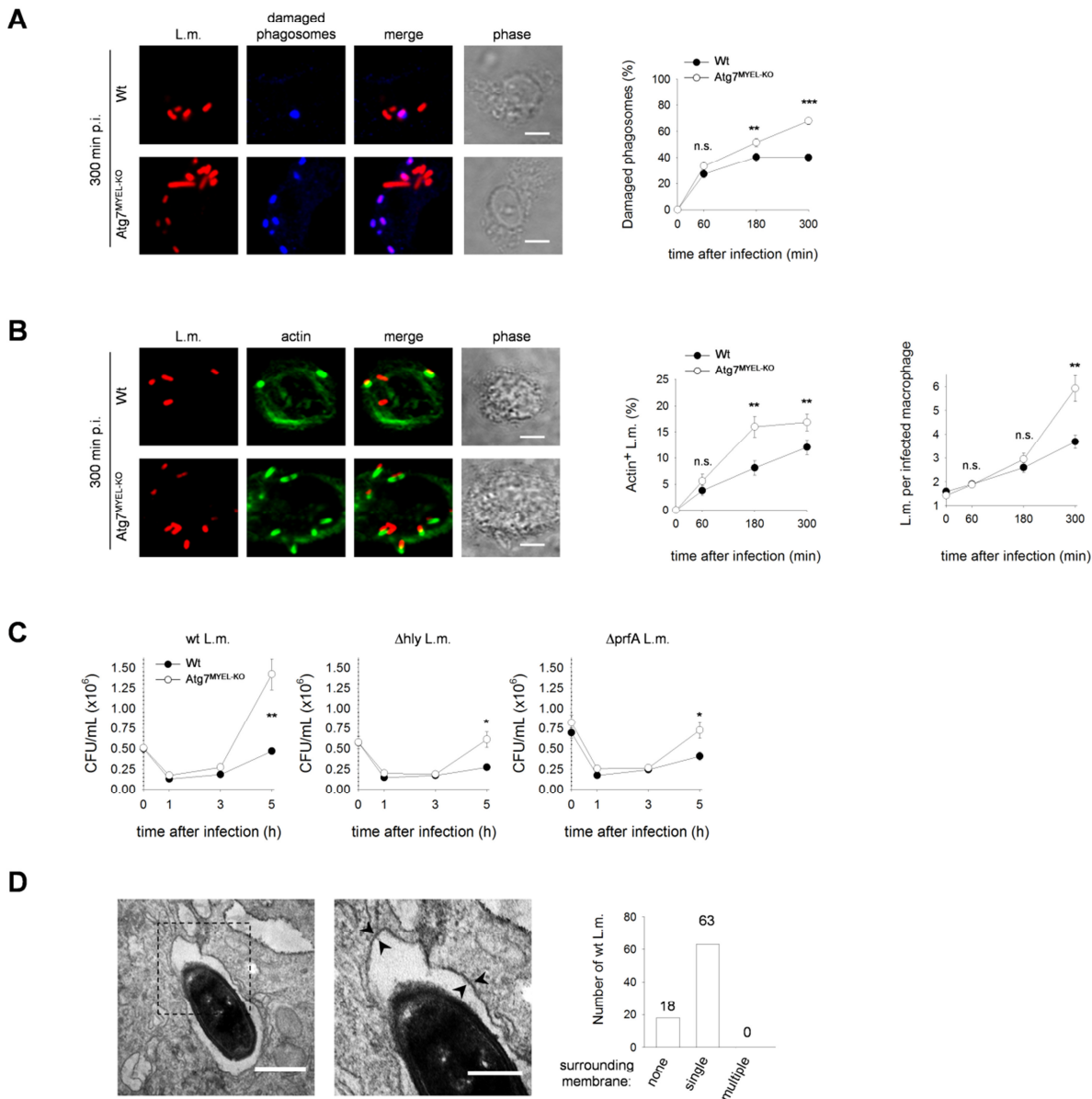
(F) Peritoneal macrophages from Wt and Atg7^{MYEL-KO} mice were infected *in vitro* with C₁₂FDG-labelled wt, Δ hly or HK L.m. at a MOI of 10. Unquenching of C₁₂FDG fluorescence by acid hydrolases was quantified. Chloroquine was used to inhibit phagosome acidification and thereby acid hydrolase activity. In addition to plotting the kinetics of C₁₂FDG fluorescence unquenching, AUC as a measure for the total amount of acid hydrolase activity was calculated. Data are shown as mean \pm SEM of five independent experiments. n.s., not significant; * p < 0.05, ** p < 0.01 and *** p < 0.001.

3.8 LAP contributes to anti-listerial immunity *in vivo*

Lysosomal acid hydrolases are crucial for effective killing of infectious pathogens in phago-lysosomes (del Cerro-Vadillo et al., 2006; Schramm et al., 2008). We therefore hypothesized that the increase in phago-lysosomal fusion mediated by LAP contributes to anti-listerial activity of macrophages. To test this hypothesis, we prolonged the duration of the *in vitro* infection of macrophages to 300 min and analyzed number of L.m. in infected cells by IFM. By using a differential staining technique, we were able to selectively stain L.m. in damaged phagosomes (Meunier et al. 2015). In addition, we used phalloidin to stain actin recruited by L.m., which escaped into the cytosol.

In Wt macrophages, about 40 % of all intracellular L.m. were contained within damaged phagosomes at 5 h after infection, whereas, in Atg7^{MYEL-KO} macrophages, more than 65 % of all intracellular L.m. were able to damage the phagosome (Fig. 10 A). Also, in Atg7^{MYEL-KO} macrophages, significantly more L.m. co-localized with actin (Fig. 10 B) indicating increased escape of L.m. into the cytoplasm. Consequently, at 5 h p.i., Atg7^{MYEL-KO} macrophages contained a significantly larger number of L.m. than Wt macrophages (Fig. 10 B). In addition, lysates of infected macrophages were plated on agar plates and number of viable L.m. indicated by bacterial colony formation was analyzed. In line with the microscopy data, these CFU experiments also showed that in Atg7^{MYEL-KO} macrophages, L.m. were able to proliferate more than in Wt macrophages. Even avirulent listeria, such as Δ hly and Δ prfA L.m., were able to proliferate in Atg7^{MYEL-KO} macrophages (Fig 10 C), while Wt macrophages efficiently restricted proliferation of Δ hly and Δ prfA L.m., indicating that LAP enhances anti-listerial activity in these cells.

Figure 10

Figure 10: LAP contributes to anti-listerial immunity *in vivo*.

- (A) Peritoneal macrophages from Wt and Atg7^{MYEL-KO} mice were infected *in vitro* with L.m. at a MOI of 1. L.m. residing in damaged phagosomes accessible to anti-L.m. antibody after differential permeabilization of the plasma membrane but not intracellular membranes were quantified by fluorescence microscopy. Representative micrographs from 5 h p.i. are shown. Data are shown as mean \pm SEM of all analyzed cells from two independent experiments. Scale bar, 4 μ m.
- (B) Peritoneal macrophages from Wt and Atg7^{MYEL-KO} mice were infected *in vitro* with L.m. at a MOI of 1. Actin⁺ L.m. and the average number of L.m. per macrophage were quantified by fluorescence microscopy. Representative micrographs from 5 h p.i. are shown. Data are shown as mean \pm SEM of all analyzed cells from three independent experiments. Scale bar, 4 μ m.
- (C) Peritoneal macrophages from Wt and Atg7^{MYEL-KO} mice were infected *in vitro* with wt, Δ hly or Δ prfA L.m. at a MOI of 1. Number of viable bacteria indicated by bacterial colony formation was determined at the indicated time points after infection. Data are shown as mean \pm SEM from two independent experiments.
- (D) Peritoneal cells were isolated from mice infected i.p. with 5×10^3 L.m. at 72 h p.i. and membrane structures surrounding L.m. were analyzed by transmission electron microscopy. Right micrograph is a magnification of the inset indicated by the black box. Arrow heads indicate single membrane. Scale bars, 500 nm and 250 nm (insert). n.s., not significant; * $p < 0.05$, ** $p < 0.01$ and *** $p < 0.001$.

To investigate whether LAP contributes to anti-listerial immunity *in vivo*, we prolonged the duration of the *in vivo* infection of mice to 72 h. At this time point, L.m. were found exclusively in vesicles surrounded by a single membrane (Fig. 10 D) and p70S6K remained phosphorylated in peritoneal cells from L.m.-infected mice (Fig. 10 E). Together, these results indicate that, even at later time points after L.m. infection, canonical autophagy is not involved in targeting of L.m..

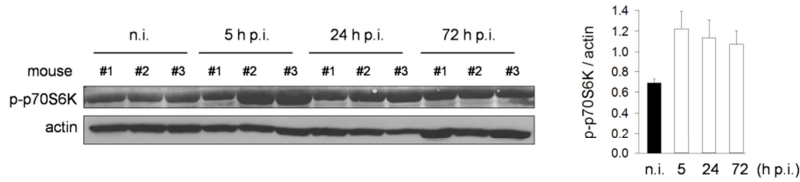
We then infected Atg7^{MYEL-KO} mice, which are deficient for LAP, intraperitoneally with L.m.. To exclude the possibility that Atg7-deficiency in myeloid cells has an impact on recruitment of immune cells during L.m. infection, we analyzed the recruitment of peritoneal cells in L.m.-infected mice by FACS. Except for increased number of neutrophils in Atg7^{MYEL-KO} mice at 72 h p.i., kinetics of immune cell recruitment were similar as in Wt mice (Fig. 10 F).

Finally, we analyzed the bacterial burden in organs of L.m.-infected mice. Liver and spleen as well as peritoneal cells from Atg7^{MYEL-KO} mice contained significantly more viable L.m. than those from Wt mice (Fig. 10 G). Notably, FIP200^{MYEL-KO} mice did not have an increased bacterial burden in liver, spleen or peritoneal cells (Fig. 10 G). These findings indicate that LAP, but not canonical autophagy, contributes to anti-listerial activity of phagocytes *in vivo*. Correspondingly, a significantly greater fraction of Atg7^{MYEL-KO} mice, but not of FIP200^{MYEL-KO} mice, succumbed to infection with L.m. (Fig. 10 H) indicating that deficiency for LAP, but not canonical autophagy, significantly increases susceptibility of mice to L.m. infection.

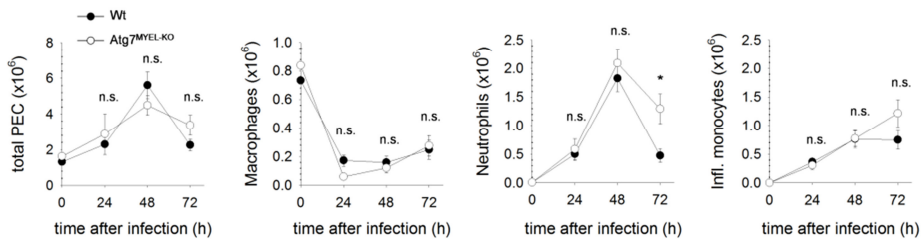
Collectively, our data show that *in vivo* L.m. are targeted by LAP and not by canonical autophagy. Mechanistically, induction of LAP is dependent on the interaction of L.m. with Mac-1, which activates ASMase and Nox2. ROS production by Nox2 is essentially required for LC3 recruitment to the phagosome. Functionally, LAP promotes fusion of L.m.-containing phagosomes with lysosomes and thereby exposure of L.m. to lysosomal acid hydrolases. Thereby, LAP enhances anti-listerial activity of macrophages and the anti-listerial immune response of mice.

Figure 10 (continued)

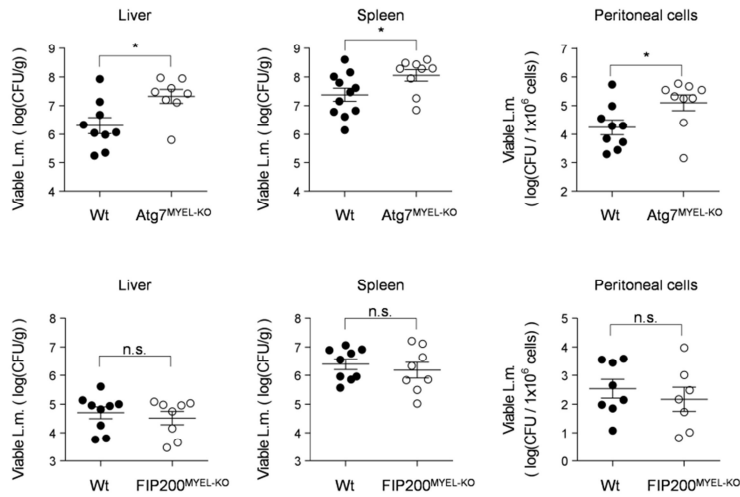
E



F



G



H

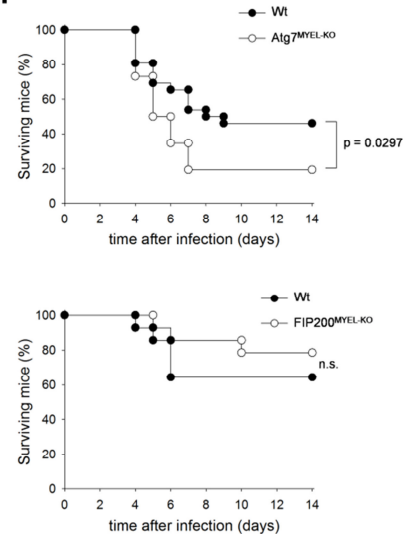


Figure 10 (continued): LAP contributes to anti-listerial immunity *in vivo*.

- (E) Phosphorylation status of p70S6K in peritoneal cells from mice infected i.p. with 7.5×10^6 wt L.m. was analyzed by Western blot and quantified by densitometry. Each lane represents an individual mouse. Data are shown as mean \pm SEM of three to six individual mice.
- (F) Wt and Atg7^{MYEL-KO} mice were infected i.p. with 7.5×10^6 wt L.m.. At the indicated time points after infection, peritoneal cells were quantified and analyzed by FACS for surface expression of F4/80, Ly6C and Ly6G. Cell numbers of F4/80⁺ macrophages, Ly6C⁺/Ly6G⁺ neutrophils and Ly6C⁺/Ly6G⁻ inflammatory monocytes were calculated by multiplying the total number of peritoneal cells with the percentage of F4/80⁺, Ly6C⁺/Ly6G⁺ or Ly6C⁺/Ly6G⁻ cells, respectively. Data are shown as mean \pm SEM of four (n.i. and 24h p.i.), eight (48 h p.i.) or eleven (72 h p.i.) mice from at least three independent experiments per time point.
- (G) Wt and Atg7^{MYEL-KO} or Wt and FIP200^{MYEL-KO} mice were infected i.p. with 5×10^3 L.m.. At 72 h p.i., viable L.m. in liver, spleen and peritoneal cells were quantified. Each dot represents an individual mouse. Data are pooled from three independent experiments and are shown as mean \pm SEM.
- (H) Survival of Wt, Atg7^{MYEL-KO} or FIP200^{MYEL-KO} mice infected i.p. with 5×10^3 L.m.. Data were pooled from four independent experiments with a total of 26 Wt and 26 Atg7^{MYEL-KO} mice, from three independent experiments with a total of 14 Wt and 14 FIP200^{MYEL-KO} mice, respectively.
n.s., not significant; * p < 0.05, ** p < 0.01 and *** p < 0.001.

3.9 Activation of LAP via Mac-1 and ASMase enhances killing of L.m. by promoting phago-lysosomal fusion.

Based on the data presented here, we propose the following model for induction of LAP in response to L.m. infection (Fig. 11). (1) Interaction of L.m. with Mac-1 induces (2) breakdown of membrane sphingomyelin into ceramide by ASMase. (3) The resulting ceramide-enriched membrane platforms facilitate aggregation of Nox2 subunits and therefore Nox2 activation. (4) Nox2-derived ROS lead to recruitment of LC3 to L.m.-containing phagosomes by LAP. (5) LAP then promotes fusion of the phagosome with lysosomes. (6) The resulting increased exposure of L.m. to lysosomal acid hydrolases enhances killing of L.m. by macrophages contributing to anti-listerial immunity in mice.

Figure 11

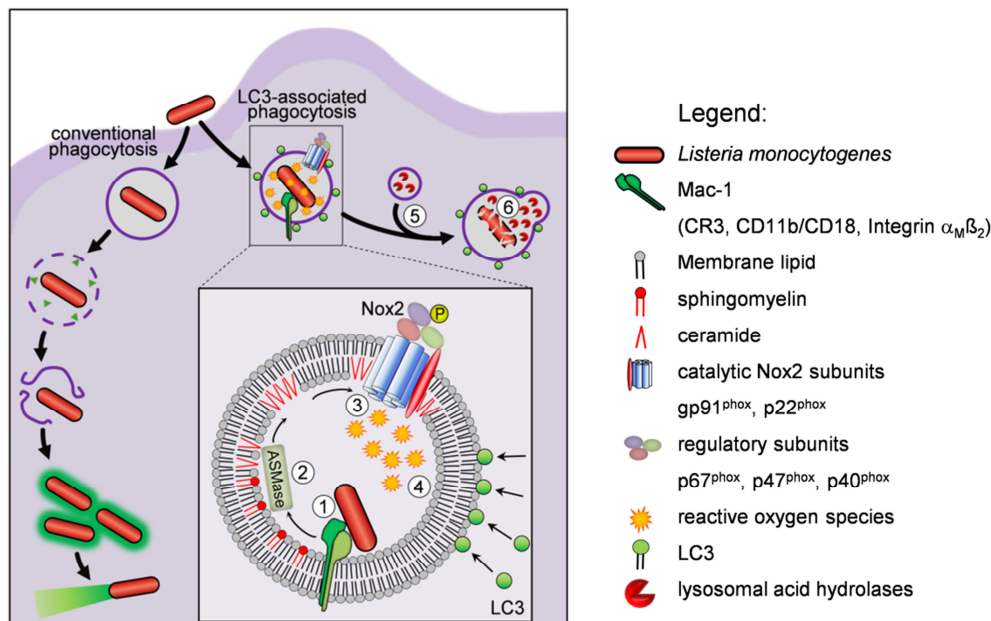


Figure 11: Model: Activation of LAP via Mac-1 and ASMase enhances killing of L.m. by promoting phago-lysosomal fusion.

Based on our data, we propose the following model for induction of LAP in response to L.m. infection:

- (1) Interaction of L.m. with Mac-1 induces ASMase activity.
- (2) ASMase cleaves the membrane lipid sphingomyelin into ceramide.
- (3) Ceramide-enriched membrane platforms facilitate Nox2 assembly. Furthermore, ASMase activity leads to phosphorylation of p40^{phox} which stabilizes the Nox2 complex.
- (4) Nox2-derived ROS lead to recruitment of LC3 to the phagosome by LAP.
- (5) LAP promotes fusion of the phagosome with lysosomes.
- (6) Exposure of L.m. to lysosomal acid hydrolases results in degradation of L.m. in the phago-lysosome.

4 Discussion

The intracellular pathogen *Listeria monocytogenes* was one of the first bacteria that have been reported to be targeted by the autophagic machinery (Rich et al., 2003). Since then, several new aspects have been added to this research field, which improved our understanding of how macrophages interact with L.m.. Particularly, Lam *et al.* have demonstrated in 2013 that *Listeria* can be targeted by LC3-associated phagocytosis (LAP), as LC3 is recruited directly to the L.m.-containing phagosome. Nevertheless, several key questions regarding the mechanisms of LC3 recruitment to single-membrane phagosomes remained to be answered, for example, which receptor induces LAP upon L.m. infection. In addition, there are some unclear points regarding the role of LAP during L.m. infection. Lam *et al.* suggested that LC3 recruitment to L.m.-containing phagosomes leads to formation of spacious *Listeria*-containing phagosomes (SLAPs), which are associated with persistent infection. By contrast, a more recent publication shows that L.m. rapidly escape from LC3-positive phagosomes and also avoid subsequent canonical autophagy in the cytosol (Mitchell et al., 2018). In order to gain new insights into autophagic targeting of L.m., both groups used *in vitro* infection models of bone marrow-derived macrophages (Mitchell et al., 2018) or RAW 264.7 cells (Lam et al., 2013). Thus, several key questions regarding autophagic targeting of L.m. *in vivo*, remained to be answered as to the discrimination between canonical autophagy and LAP and their relative functional consequences for promoting elimination or persistence of L.m..

To investigate if LAP does play a role in immunity to L.m. *in vivo*, we used intraperitoneal L.m. infection of mice to model infection of tissue-resident macrophages. We demonstrated that, *in vivo*, L.m. are exclusively targeted by LAP, which promotes fusion of L.m.-containing phagosomes with lysosomes and thereby contributes to anti-listerial immunity.

In addition, by using a respective panel of knockout mice, we identified the mechanism for induction of LAP in response to L.m. infection. Specifically, we show that binding or recognition of L.m. by the β_2 integrin Mac-1 induces activation of ASMase. ASMase activity is essentially required for Nox2 assembly and subsequent ROS production, which are a prerequisite for LC3 recruitment to L.m.-containing phagosomes. LC3-positive phagosomes then fuse with lysosomes, which increases exposure of L.m. to bactericidal lysosomal acid hydrolases, thereby enhancing anti-listerial immunity in mice.

Several independent lines of evidence indicate that LC3 targeting of L.m. represents LAP and not canonical autophagy: 1) L.m. were found exclusively in single-membrane phagosomes or in the cytosol, but not in double- or multi-membrane vesicles. 2) mTOR remained active during infection of mice with L.m., while pharmacological activation of canonical autophagy with rapamycin, inactivated mTOR. 3) LC3 recruitment was independent of the autophagy initiation complex components Ulk1/2 and FIP200. 4) LC3 recruitment did not require bacterial LLO- and/or phospholipases-inflicted damage to the phagosomal membrane, i.e. access of L.m. to the cytosol. 5) LC3 recruitment to L.m.-containing phagosomes required ROS production by Nox2. These all are hallmarks of LAP (Huang et al., 2009; Lam et al., 2013; Martinez et al., 2015). Thus, our data indicate that, *in vivo*, L.m. are exclusively targeted by LAP.

Several different receptors inducing LAP have been identified: In the case of apoptotic cells, the membrane lipid phosphatidylserine, which faces only the cytosolic side of the plasma membrane in healthy cells, is recognized by the receptor TIM4, which triggers LAP induction (Martinez et al., 2011). In the case of fungal particles, the receptor Dectin-1 recognizes β -glucans in fungal cell walls and triggers LAP (Ma et al. 2012). Regarding Listeria, it has been previously reported that TLR2 and NOD1/2 are required for autophagic targeting of L.m. (Anand et al., 2011), but it remained unknown, whether TLR2 and NOD1/2 are required for induction of LAP or rather for canonical autophagy.

We now demonstrate that targeting of L.m. by LAP is induced via the β_2 integrin Mac-1. Deficiency for the CD11b subunit of Mac-1 markedly impaired recruitment of LC3 to L.m.-containing phagosomes indicating that interaction of L.m. with Mac-1 is required for LAP induction. Of note, LC3 recruitment is not completely abrogated in CD11b-deficient macrophages, which indicates that Mac-1 is not the sole receptor inducing LAP in response to L.m. infection. We can exclude that TLR2 and NOD1/2 are required for LAP induction of L.m., since LC3 recruitment to L.m.-containing phagosomes was unaltered in peritoneal macrophages from TLR2^{-/-}, MyD88^{-/-} and NOD2^{-/-} mice. As, macrophages express almost 200 different receptors (Mitchell et al., 2016; Ley et al., 2016), there is a high probability that several receptors can induce LAP in response to bacterial infection. These receptors and the ligands, which are involved, remain to be identified.

Mechanistically, Mac-1 induced LC3 recruitment to L.m.-containing phagosomes by activating Nox2. Deficiency for CD11b markedly impaired ROS production by L.m.-infected macrophages showing that Nox2 activation in response to L.m. infection largely depends on Mac-1 (Gluschko and Herb et al., 2018). In detail, interaction of L.m. with Mac-1 resulted in activation of ASMase, which was a prerequisite for Nox2 activation. Mac-1-deficient macrophages largely failed to activate ASMase after L.m. infection and deficiency for ASMase markedly impaired Nox2 activation. ASMase is known to be an important regulator of Nox2 activity because ceramide-enriched membrane platforms generated by ASMase facilitate aggregation of Nox2 subunits and therefore Nox2 activation (Zhang et al., 2008). Moreover, ASMase activity was impaired in Nox2-deficient macrophages indicating that Nox2-derived ROS amplify ASMase activity in a positive feedback loop (Gluschko and Herb et al., 2018). A similar positive feedback loop has been reported to induce apoptosis in *Pseudomonas aeruginosa*-

infected macrophages (Zhang et al., 2008). Upon L.m. infection, however, we show here that the Mac-1-induced interplay between ASMase and Nox2 is required for induction of LAP.

Like LC3 recruitment, Nox2 activation was not completely impaired in Mac-1-deficient macrophages (Gluschko and Herb et al., 2018) indicating that Mac-1 is not the sole receptor inducing Nox2 activation and subsequent targeting of L.m. by LAP. The receptor(s) cooperating with Mac-1 in activating Nox2 and LAP, however, remain to be identified.

A surprising finding of this work was that LAP *in vivo* is completely independent of L.m. virulence factors, since LC3 recruitment to prfA- or LLO-deficient L.m. was not altered. This is in discrepancy to BMDM and macrophage-like cell lines such as RAW 264.7 cells in which LLO-inflicted phagosomal damage is strictly required for LC3 recruitment to L.m. (Lam et al., 2013; Meyer-Morse et al., 2010). Yet, both in BMDM and RAW 264.7 cells (Lam et al., 2013) and in peritoneal macrophages, ROS production by Nox2 is a major factor in LAP induction.

BMDM have been described as not yet fully matured macrophages (Wang, Yu et al. 2013). They express lower amounts of surface molecules, e. g. CD86 and MHC class II, than mature macrophages such as peritoneal macrophages. Instead, BMDM express higher levels of CD115 and GR-1, which are mostly expressed on less differentiated cells, e. g. precursors of monocytes (Wang, Yu et al. 2013). Indeed, we observed that peritoneal macrophages produce significantly larger amounts of ROS by Nox2 than BMDM (Gluschko, Herb et al., 2018). The most likely reason for this is that peritoneal macrophages, in comparison to BMDM, have higher protein levels of Nox2 as well as of the upstream activation factors CD11b and ASMase (Gluschko, Herb et al., 2018). These findings provide a plausible explanation for the discrepancies between data using BMDM and those using resident tissue macrophages. It would be interesting to analyze whether stimulation of BMDM with cytokines or bacterial PAMPs upregulates expression of Nox2 and thereby increases ROS production in response to L.m.

infection. If that is the case, it would be interesting to investigate whether increased ROS production in BMDM enables the induction of LAP in response to avirulent listeria as in peritoneal macrophages.

One important key question that remains to be solved, is how exactly Nox2-derived ROS induce LC3 recruitment to L.m.-containing phagosomes during LAP. ROS have been implicated in various cell signaling pathways that involve the reversible oxidation and reduction of specific reactive Cys residues (Holmstrom and Finkel, 2014). Therefore, it is possible that Nox2-derived ROS directly act as signaling molecules by modifying redox-sensitive components of the autophagic machinery such as Atg4 (Scherz-Shouval et al. 2007). By contrast, ROS can damage not only microbial but also cellular molecules, including membrane lipids of the phagosomal membrane. Therefore, it is tempting to speculate that ROS-induced membrane damage is the reason for recruitment of LC3 to the phagosomal membrane, as it is the case for pore-forming toxins such as LLO (Meyer-Morse et al. 2010).

With regard to the role of LAP in immunity to L.m. infection, we show that Mac-1-induced LAP contributes to anti-listerial immunity in mice. Atg7^{MYEL-KO} mice, which are deficient for autophagy and LAP, were significantly more susceptible to L.m. infection. They had an increased bacterial load in their organs, and peritoneal macrophages of these mice contained significantly more viable bacteria. By contrast, FIP200^{MYEL-KO} mice, which are deficient for autophagy but not for LAP, showed no increased susceptibility to L.m. infection. In addition, even at later time points after infection of wild type mice, mTOR remained active and L.m. exclusively resided within single-membrane vesicles. Together, these data indicate that only LAP, but not canonical autophagy, contributes to elimination of L.m. by macrophages.

Mechanistically, the transfer of lysosomal acid hydrolases into L.m.-containing phagosomes by phago-lysosomal fusion is of critical importance for anti-listerial activity of macrophages (del Cerro-Vadillo et al., 2006; Schramm et al., 2008), and LAP has been shown to promote fusion of phagosomes with lysosomes (Mehta et al., 2014). We show here that fusion of L.m.-containing phagosomes with lysosomes was significantly impaired in LAP-deficient macrophages. This resulted in reduced exposure of L.m. to lysosomal acid hydrolases and allowed escape of L.m. from the phagosome into the cytosol. In the cytosol, L.m. proliferated and induced actin polymerization for actin-based motility and subsequent infection of neighboring cells. Thus, our data clearly show that, by promoting fusion of L.m.-containing phagosomes with lysosomes and thereby exposure of L.m. to lysosomal acid hydrolases, LAP enhances anti-listerial activity of macrophages and enhances the anti-listerial immune response of mice. This is in line with data from other infection models, where LAP has been reported to enhance anti-microbial activity (Huang et al., 2009; Gong et al., 2011; Tam et al., 2014; Martinez et al., 2015; Boonhok et al., 2016) and strongly argues against the idea that LAP may favor persistence of L.m.. Nevertheless, one important question that remains unsolved is how LC3 promotes fusion with lysosomes. As LC3 can be/has originally been identified as a protein associated with microtubules, it is tempting to speculate that LC3 may be involved in the transport of the phagosome along microtubules. Indeed, Ma *et al.* have reported that accelerated fusion of phagosomes with lysosomes might be due to more efficient transport along microtubules via LC3 binding to FYVE and coiled-coil domain containing 1 (FYCO1) protein (Ma et al. 2014). Nevertheless, the detailed mechanism how interaction of LC3 and FYVE or FYCO1 accelerates transport of phagosomes requires further investigation.

Interestingly, in dendritic cells, an opposing role for LAP has been described. Here, LC3-positive phagosomes were found to be long-lived structures with delayed recruitment of lysosomes. This leads to stabilization of the cargo and prolongs antigen presentation on major histocompatibility complex (MHC) class II molecules (Ma et al. 2012; Romao et al. 2013). The

above finding implies that LAP can have different functions depending on the cell type and the cargo of the phagosome. The molecular mechanisms underlying these different roles of LAP, however, remain to be elucidated.

Overall, the vast majority of publications demonstrate that LAP has beneficial effects for the cell and the whole organism and that deficiency for LAP is associated with inflammation, auto-antibody generation (Martinez et al., 2016) and increased susceptibility to bacterial and fungal infections (Huang et al., 2009; Tam et al., 2014). Since LAP can be induced by lysosomotropic drugs (Florey et al. 2015), it should be investigated in the future, whether lysosomotropic properties of certain detergents might be of use in activation of LAP and improvement of the immune response during bacterial and fungal infections.

5 References

- Anand, P. K., S. W. Tait, et al. (2011). "TLR2 and RIP2 pathways mediate autophagy of *Listeria monocytogenes* via extracellular signal-regulated kinase (ERK) activation." J Biol Chem 286(50): 42981-42991.
- Baxt L.A., Goldberg M.B., (2014). Host and bacterial proteins that repress recruitment of LC3 to *Shigella* early during infection. PLoS One, 9, p. e94653, 10.1371/journal.pone.0094653
- Bedard, K. and Krause, K.H. (2007) The NOX family of ROS-generating NADPH oxidases: physiology and pathophysiology. Physiol. Rev. 87, 245–313
- Birmingham, C. L., V. Canadien, et al. (2008). "Listeriolysin O allows *Listeria monocytogenes* replication in macrophage vacuoles." Nature 451(7176): 350-354.
- Boonhok, R., et al. (2016). LAP-like process as an immune mechanism downstream of IFN-gamma in control of the human malaria *Plasmodium vivax* liver stage. Proc Natl Acad Sci U S A 113, E3519-E3528.
- Brown, E. J., M. W. Albers, et al. (1994). "A mammalian protein targeted by G1-arresting rapamycin-receptor complex." Nature 369(6483): 756-758.
- Bustamante J, et al. (2011). Germline CYBB mutations that selectively affect macrophages in kindreds with X-linked predisposition to tuberculous mycobacterial disease. Nat Immunol.;12:213–221.
- Carneseccchi, S., et al. (2011). A key role for NOX4 in epithelial cell death during development of lung fibrosis. Antioxidants & redox signaling. 15(3), 607-619. Published online 2011/03/12 DOI: 10.1089/ars.2010.3829.
- Cemma, M. and J. H. Brumell (2012). "Interactions of pathogenic bacteria with autophagy systems." Curr Biol 22(13): R540-545.
- Chessa, T.A., et al. (2010). Phosphorylation of threonine 154 in p40phox is an important physiological signal for activation of the neutrophil NADPH oxidase. Blood 116, 6027-6036.
- Clausen, B.E., et al. (1999). Conditional gene targeting in macrophages and granulocytes using LysMcre mice. Transgenic Research. 8(4), 265-277. DOI: Doi 10.1023/A:1008942828960.
- del Cerro-Vadillo, E., et al. (2006). Cutting edge: a novel nonoxidative phagosomal mechanism exerted by cathepsin-D controls *Listeria monocytogenes* intracellular growth. J Immunol. 176(3), 1321-1325.
- Dortet, L., S. Mostowy, et al. (2011). "Recruitment of the major vault protein by InlK: a *Listeria monocytogenes* strategy to avoid autophagy." PLoS Pathog 7(8): e1002168.

- Drevets, D.A., Leenen, P.J.M., and Campbell, P.A. (1993). Complement Receptor Type-3 (Cd11b/Cd18) Involvement Is Essential for Killing of Listeria-Monocytogenes by Mouse Macrophages. J Immunol. 151(10), 5431-5439.
- Ehlers, M.R., (2000). CR3: a general purpose adhesion-recognition receptor essential for innate immunity. Microbes Infect. 2(3), 289-294. Published online 2000/04/12.
- Eskelinen, E. L. and P. Saftig (2009). "Autophagy: a lysosomal degradation pathway with a central role in health and disease." Biochim Biophys Acta 1793(4): 664-673.
- Florey, O. and M. Overholtzer (2012). "Autophagy proteins in macroendocytic engulfment." Trends Cell Biol 22(7): 374-380.
- Florey O., et al. (2015). V-ATPase and osmotic imbalances activate endolysosomal LC3 lipidation. Autophagy; 11:88-99; PMID: 25484071; <http://dx.doi.org/10.4161/15548627.2014.984277>
- Freitag, N. E., G. C. Port, et al. (2009). "Listeria monocytogenes - from saprophyte to intracellular pathogen." Nat Rev Microbiol 7(9): 623-628.
- Gan, B., et al. (2006). Role of FIP200 in cardiac and liver development and its regulation of TNF α and TSC-mTOR signaling pathways. J Cell Biol. ;175(1):121-33. doi:10.1083/jcb.200604129.
- Gao H. M., et al. (2011). HMGB1 acts on microglia Mac1 to mediate chronic neuroinflammation that drives progressive neurodegeneration. J. Neurosci. 31: 1081-1092.
- Gavazzi, G., et al.(2006). Decreased blood pressure in NOX1-deficient mice. FEBS letters. 580(2), 497-504. Published online 2006/01/03 DOI: 10.1016/j.febslet.2005.12.049.
- Gluschko, A., Herb, M., et al. (2018). The beta2 Integrin Mac-1 Induces Protective LC3-Associated Phagocytosis of Listeria monocytogenes. Cell host & microbe 23, 324-337 e325.
- Goldberg, M. B. (2001). "Actin-based motility of intracellular microbial pathogens." Microbiol Mol Biol Rev 65(4): 595-626, table of contents.
- Gulbins, E. and P. L. Li (2006). "Physiological and pathophysiological aspects of ceramide." Am J Physiol Regul Integr Comp Physiol 290(1): R11-26.
- Gong L. et al., (2011). The Burkholderia pseudomallei type III secretion system and BopA are required for evasion of LC3-associated phagocytosis. PLoS One, p. 6, 10.1371/journal.pone.0017852
- Hamasaki, M., N. Furuta, et al. (2013). "Autophagosomes form at ER-mitochondria contact sites." Nature 495(7441): 389-393.
- Holmström, K.M., and Finkel, T. (2014). Cellular mechanisms and physiological consequences of redox-dependent signalling. Nature reviews Molecular cell biology 15, 411-421.

- Horinouchi, K., et al. (1995). Acid sphingomyelinase deficient mice: a model of types A and B Niemann-Pick disease. Nat Genet. 10(3), 288-293. Published online 1995/07/01 DOI: 10.1038/ng0795-288.
- Huang, J., and Brumell, J.H. (2014). Bacteria-autophagy interplay: a battle for survival. Nat Rev Microbiol. 12(2), 101-114. Published online 2014/01/05 DOI: 10.1038/nrmicro3160.
- Huang, J., V. Canadien, et al. (2009). "Activation of antibacterial autophagy by NADPH oxidases." Proc Natl Acad Sci U S A 106(15): 6226-6231.
- Hubber A. (2017). Bacterial secretion system skews the fate of Legionella-containing vacuoles towards LC3-associated phagocytosis. Sci. Rep., 7, p. 44795, 10.1038/srep44795
- Klionsky, D. J., F. C. Abdalla, et al. (2012). "Guidelines for the use and interpretation of assays for monitoring autophagy." Autophagy 8(4): 445-544.
- Klionsky, D.J., Abdelmohsen, K., Abe, A., Abedin, M.J., Abeliovich, H., Arozena, A.A., Adachi, H., Adams, C.M., Adams, P.D., Adeli, K., et al. (2016). Guidelines for the use and interpretation of assays for monitoring autophagy (3rd edition). Autophagy 12, 1-222.
- Köster, S., et al. (2017). Mycobacterium tuberculosis is protected from NADPH oxidase and LC3-associated phagocytosis by the LCP protein CpsA. Proc Natl Acad Sci U S A, pp. 1-10, 10.1073/pnas.1707792114
- Lai, S.-c. and R. J. Devenish (2012). "LC3-Associated Phagocytosis (LAP): Connections with Host Autophagy." Cells 1(3): 396-408.
- Lam, G. Y., M. Cemma, et al. (2013). "Host and bacterial factors that regulate LC3 recruitment to Listeria monocytogenes during the early stages of macrophage infection." Autophagy 9(7).
- Lerena, M. C., C. L. Vazquez, et al. (2010). "Bacterial pathogens and the autophagic response." Cell Microbiol 12(1): 10-18.
- Levade, T. and J. P. Jaffrezou (1999). "Signalling sphingomyelinases: which, where, how and why?" Biochim Biophys Acta 1438(1): 1-17.
- Levine, B., N. Mizushima, et al. (2011). "Autophagy in immunity and inflammation." Nature 469(7330): 323-335.
- Ley, K., et al. (2016). How Mouse Macrophages Sense What Is Going On. Front Immunol. 7(204), 204. DOI: 10.3389/fimmu.2016.00204.
- Ligeon L.A. et al., (2014). Role of VAMP3 and VAMP7 in the commitment of Yersinia pseudotuberculosis to LC3-associated pathways involving single- or double-membrane vacuoles. Autophagy, 10 (2014), pp. 1588-1602.
- Ma, J., C. Becker, et al. (2012). "Dectin-1-triggered recruitment of light chain 3 protein to phagosomes facilitates major histocompatibility complex class II presentation of fungal-derived antigens." J Biol Chem 287(41): 34149-34156.

- Ma J, Becker C, et al. (2014). Cutting edge: FYCO1 recruitment to dectin-1 phagosomes is accelerated by light chain 3 protein and regulates phagosome maturation and reactive oxygen production. J Immunol 192:1356–60. doi:10.4049/jimmunol.1302835
- Martinez, J., J. Almendinger, et al. (2011). "Microtubule-associated protein 1 light chain 3 alpha (LC3)-associated phagocytosis is required for the efficient clearance of dead cells." Proc Natl Acad Sci U S A 108(42): 17396-17401.
- Martinez, J., et al. (2015). Molecular characterization of LC3-associated phagocytosis reveals distinct roles for Rubicon, NOX2 and autophagy proteins. Nat Cell Biol. 17(7), 893-906. Published online 2015/06/23 DOI: 10.1038/ncb3192.
- Martinez, J., et al. (2016). Noncanonical autophagy inhibits the autoinflammatory, lupus-like response to dying cells. Nature 533, 115.
- Mehta, P., Henault, J., Kolbeck, R., and Sanjuan, M.A. (2014). Noncanonical autophagy: one small step for LC3, one giant leap for immunity. Curr Opin Immunol. 26, 69-75. Published online 2014/02/22 DOI: 10.1016/j.coi.2013.10.012.
- Meunier, E., and Broz, P. (2015). Quantification of cytosolic vs. vacuolar salmonella in primary macrophages by differential permeabilization. J. Vis. Exp. 101:e52960. doi: 10.3791/52960
- Meyer-Morse, N., J. R. Robbins, et al. (2010). "Listeriolysin O is necessary and sufficient to induce autophagy during *Listeria monocytogenes* infection." PLoS One 5(1): e8610.
- Mitchell, G., Chen, C., & Portnoy, D. A. (2016). Strategies used by bacteria to grow in macrophages. Microbiology Spectrum, 4(3), 10.1128/microbiolspec.MCHD–0012–2015.
- Mitchell, G., et al. (2018). *Listeria monocytogenes* triggers noncanonical autophagy upon phagocytosis, but avoids subsequent growth-restricting xenophagy. Proceedings of the National Academy of Sciences 115, E210-E217.
- Mizushima, N., et al. (2004). In vivo analysis of autophagy in response to nutrient starvation using transgenic mice expressing a fluorescent autophagosome marker. Molecular biology of the cell. 15(3), 1101-1111.
- Ogawa, M., Y. Yoshikawa, et al. (2011). "Autophagy targeting of *Listeria monocytogenes* and the bacterial countermeasure." Autophagy 7(3): 310-314.
- Ogawa, M., T. Yoshimori, et al. (2005). "Escape of intracellular *Shigella* from autophagy." Science 307(5710): 727-731.
- Peters, C. et al. (2003). Tailoring host immune responses to *Listeria* by manipulation of virulence genes -- the interface between innate and acquired immunity. FEMS immunology and medical microbiology 35, 243-253.
- Pollock, J.D., et al. (1995). Mouse model of X-linked chronic granulomatous disease, an inherited defect in phagocyte superoxide production. Nat Genet. 9(2), 202-209. Published online 1995/02/01 DOI: 10.1038/ng0295-202.

- Py, B. F., M. M. Lipinski, et al. (2007). "Autophagy limits *Listeria monocytogenes* intracellular growth in the early phase of primary infection." Autophagy 3(2): 117-125.
- Ray, K., B. Marteyn, et al. (2009). "Life on the inside: the intracellular lifestyle of cytosolic bacteria." Nat Rev Microbiol 7(5): 333-340.
- Rich, K.A., Burkett, C., and Webster, P. (2003). Cytoplasmic bacteria can be targets for autophagy. Cell Microbiol 5, 455-468.
- Romao S., et al. (2013). Autophagy proteins stabilize pathogen-containing phagosomes for prolonged MHC II antigen processing J Cell Biol 203 757 66 doi: 10.1083/jcb.201308173.
- Sanjuan, M.A., et al. (2007). Toll-like receptor signalling in macrophages links the autophagy pathway to phagocytosis. Nature 450, 1253-1257.
- Scherz-Shouval, R., et al. (2007). Reactive oxygen species are essential for autophagy and specifically regulate the activity of Atg4. The EMBO Journal, 26(7), 1749–1760. <http://doi.org/10.1038/sj.emboj.7601623>
- Schramm, M., J. Herz, et al. (2008). "Acid sphingomyelinase is required for efficient phagolysosomal fusion." Cell Microbiol 10(9): 1839-1853.
- Singel, K. L., & Segal, B. H. (2016). NOX2-dependent regulation of inflammation. Clinical Science (London, England : 1979), 130(7), 479–490. <http://doi.org/10.1042/CS20150660>
- Solovjov D. A., E. Pluskota, E. F. Plow. (2005). Distinct roles for the alpha and beta subunits in the functions of integrin alphaMbeta2. J. Biol. Chem. 280: 1336–1345.
- Tam JM, Mansour MK, Khan NS, Seward M, Puranam S, Tanne A, et al. Dectin-1-dependent LC3 recruitment to phagosomes enhances fungicidal activity in macrophages. J Infect Dis (2014) 210:1844–54. [10.1093/infdis/jiu290](https://doi.org/10.1093/infdis/jiu290)
- Tindwa, H., Jo, Y.H., Patnaik, B.B., Lee, Y.S., Kang, S.S., and Han, Y.S. (2015). Molecular cloning and characterization of autophagy-related gene TmATG8 in *Listeria*-invaded hemocytes of *Tenebrio molitor*. Dev Comp Immunol 51, 88-98.
- Truman, J. P., M. M. Al Gadban, et al. (2011). "Acid sphingomyelinase in macrophage biology." Cell Mol Life Sci 68(20): 3293-3305.
- Unanue, E.R. (1997). Inter-relationship among macrophages, natural killer cells and neutrophils in early stages of *Listeria* resistance. Curr Opin Immunol, 9, pp. 35-43
- Utermohlen, O., J. Herz, et al. (2008). "Fusogenicity of membranes: the impact of acid sphingomyelinase on innate immune responses." Immunobiology 213(3-4): 307-314.
- Utermohlen, O., U. Karow, et al. (2003). "Severe impairment in early host defense against *Listeria monocytogenes* in mice deficient in acid sphingomyelinase." J Immunol 170(5): 2621-2628.
- W. and D. J. Klionsky (2003). "The molecular mechanism of autophagy. Mol Med 9(3-4): 65-76.

- Wang, C., X. Yu, et al. (2013). "Characterization of murine macrophages from bone marrow, spleen and peritoneum." *BMC Immunol* 14: 6.
- Weiss, G., & Schaible, U. E. (2015). Macrophage defense mechanisms against intracellular bacteria. *Immunological Reviews*, 264(1), 182–203.
- Wiegmann, K., et al. (1994). Functional dichotomy of neutral and acidic sphingomyelinases in tumor necrosis factor signaling. *Cell*. 78(6), 1005-1015. Published online 1994/09/23.
- Wong, P. M., C. Puente, et al. (2013). "The ULK1 complex: sensing nutrient signals for autophagy activation." *Autophagy* 9(2): 124-137.
- Yang, Z. and D. J. Klionsky (2010). "Mammalian autophagy: core molecular machinery and signaling regulation." *Curr Opin Cell Biol* 22(2): 124-131.
- Yano, T., Mita, S., Ohmori, H., Oshima, Y., Fujimoto, Y., Ueda, R., Takada, H., Goldman, W.E., Fukase, K., Silverman, N., et al. (2008). Autophagic control of listeria through intracellular innate immune recognition in drosophila. *Nat Immunol* 9, 908-916.
- Yoshikawa, Y., M. Ogawa, et al. (2009). "Listeria monocytogenes ActA-mediated escape from autophagic recognition." *Nat Cell Biol* 11(10): 1233-1240.
- Yuk, J. M., T. Yoshimori, et al. (2012). "Autophagy and bacterial infectious diseases." *Exp Mol Med* 44(2): 99-108.
- Zhang, Y., Li, X., Carpinteiro, A., and Gulbins, E. (2008). Acid sphingomyelinase amplifies redox signaling in *Pseudomonas aeruginosa*-induced macrophage apoptosis. *Journal of immunology* 181, 4247-4254.
- Zhang, X., R. Goncalves, et al. (2008). "The isolation and characterization of murine macrophages." *Curr Protoc Immunol* Chapter 14: Unit 14 11.
- Zhao, Z., et al. (2008). Autophagosome-independent essential function for the autophagy protein Atg5 in cellular immunity to intracellular pathogens. *Cell Host Microbe* 4, 458-469.
- Zheng, Y. T., S. Shahnazari, et al. (2009). "The adaptor protein p62/SQSTM1 targets invading bacteria to the autophagy pathway." *J Immunol* 183(9): 5909-5916.
- Zhou, H., et al., (2013). CD11b/CD18 (Mac-1) Is a Novel Surface Receptor for Extracellular Double-Stranded RNA To Mediate Cellular Inflammatory Responses. *The Journal of Immunology* 190, 115.

Summary

Listeria monocytogenes (L.m.) are targeted by the autophagic machinery, however, the molecular mechanisms involved and the functional consequences for anti-listerial immunity remained unknown. Here, we use an *in vivo* mouse infection model to show that L.m. infection of tissue macrophages evokes LC3-associated phagocytosis (LAP), but not canonical autophagy, and that targeting of L.m. by LAP is required for anti-listerial immunity. Furthermore, by employing a group of genetically deficient mouse lines, we delineate the molecular pathway leading to induction of LAP in response to L.m. infection and the mechanisms underlying the anti-listerial function of LAP. Induction of LAP in response to L.m. infection is not initiated by TLR2 or MyD88 dependent signaling pathways, but by the β_2 integrin Mac-1 (CR3, integrin $\alpha_M\beta_2$). Interaction of L.m. with Mac-1 results in activation of acid sphingomyelinase, which is essentially required for assembly and activation of the phagocyte NADPH oxidase Nox2. Subsequent production of reactive oxygen species by Nox2 triggers LC3 recruitment to L.m.-containing phagosomes. LC3-positive L.m.-containing phagosomes fuse with lysosomes, which increases exposure of L.m. to bactericidal acid hydrolases and thereby enhances anti-listerial activity of macrophages and immunity of mice.

Zusammenfassung

Listeria monocytogenes (L.m.) kann durch Autophagie getargetet werden, allerdings sind die dafür verantwortlichen molekularen Mechanismen und die funktionellen Konsequenzen für die anti-listerielle Immunantwort noch unbekannt. In dieser Arbeit verwenden wir ein *In-vivo*-Infektionsmodell von Mäusen, um zu zeigen, dass L.m.- Infektion von Gewebsmakrophagen LC3-assoziierte Phagozytose (LAP), nicht aber kanonische Autophagie, induziert und dass das Targeting von L.m. durch LAP für die anti-listerielle Immunantwort erforderlich ist. Durch die Verwendung verschiedener genetisch defizienter Mauslinien haben wir außerdem die zur Induktion von LAP als Reaktion auf die L.m.-Infektion führende molekulare Signalkaskade aufgeklärt. Wir zeigen, dass die LAP-Induktion nicht durch TLR2- oder MyD88-abhängige Signalwege, sondern durch das β_2 -Integrin Mac-1 (CR3, Integrin $\alpha M\beta 2$), vermittelt wird. Die Interaktion von L.m. mit Mac-1 führt zur Aktivierung der sauren Sphingomyelinase, welche für die Aktivierung der NADPH-Oxidase Nox2 benötigt wird. Die daraus resultierende Produktion von reaktiven Sauerstoffspezies durch Nox2 initiiert die Rekrutierung von LC3 zu L.m.-enthaltenden Phagosomen. LC3-positive, L.m.-enthaltende Phagosomen fusionieren verstärkt mit Lysosomen, wodurch die Exposition von L.m. gegenüber bakteriziden Verdauungsenzymen erhöht und die anti-listerielle Aktivität von Makrophagen und die Immunität von Mäusen verbessert wird.

Danksagung

An erster Stelle gilt mein Dank Herrn Dr. Michael Schramm, dafür, dass er mich in dieses Projekt involviert hat und mich während der gesamten Promotion, angefangen bei der Einarbeitung im Labor bis zur kritischen Durchsicht dieser Arbeit, sehr engagiert betreut und unterstützt hat.

Bei Prof. Dr. Thorsten Hoppe möchte ich mich für die freundliche Übernahme des Erstgutachtens meiner Dissertation bedanken.

Prof. Dr. Krönke danke ich für die Möglichkeit diese Arbeit an seinem Institut anzufertigen und für die freundliche Übernahme des Zweitgutachtens.

Außerdem gilt mein Dank Herrn Prof. Dr. Neiss für die Gelegenheit TEM-Aufnahmen an seinem Institut anzufertigen und Frau Petra Müller für die freundliche Unterstützung dabei.

Katja Wiegmann danke ich für die für die zahlreiche Unterstützung insbesondere bei den ASMase-Aktivitätsmessungen.

Prof. Dr. Olaf Utermöhlen und Dr. Oleg Krut danke ich für die fachlichen Gespräche, Ratschläge und Anmerkungen, die diese Arbeit durch neue Denkansätze und Ideen weitergebracht haben.

Ulrike Karow, Sandra Schramm, Alzbeta Machova und Arlette Paillard bin ich sehr dankbar für die zahlreiche Unterstützung, Hilfsbereitschaft sowie die konstruktive und angenehme Zusammenarbeit.

Zum Schluss möchte ich mich ganz herzlich bei meinem Laborpartner Marc Herb für die wunderbare Zusammenarbeit und gute Freundschaft bedanken.

Erklärung

Ich versichere, dass ich die von mir vorgelegte Dissertation selbständig angefertigt, die benutzten Quellen und Hilfsmittel vollständig angegeben und die Stellen der Arbeit - einschließlich Tabellen, Karten und Abbildungen -, die anderen Werken im Wortlaut oder dem Sinn nach entnommen sind, in jedem Einzelfall als Entlehnung kenntlich gemacht habe; dass diese Dissertation noch keiner anderen Fakultät oder Universität zur Prüfung vorgelegen hat; dass sie - abgesehen von unten angegebenen Teilpublikationen - noch nicht veröffentlicht worden ist sowie, dass ich eine solche Veröffentlichung vor Abschluss des Promotionsverfahrens nicht vornehmen werde. Die Bestimmungen der Promotionsordnung sind mir bekannt. Die von mir vorgelegte Arbeit ist von Herrn Dr. Michael Schramm betreut worden.

Teilpublikationen

Alexander Gluschko, Marc Herb, Katja Wiegmann, Oleg Krut, Wolfram F. Neiss, Olaf Utermöhlen, Martin Krönke, Michael Schramm. **The β_2 Integrin Mac-1 Induces Protective LC3-Associated Phagocytosis of *Listeria monocytogenes*.** *Cell Host & Microbe* (2018) 23, 324-337 e325. DOI: <https://doi.org/10.1016/j.chom.2018.01.018>

Marc Herb, Alexander Gluschko and Michael Schramm. **LC3-associated phagocytosis initiated by the β_2 integrin Mac-1 enhances immunity to *Listeria monocytogenes*.** *Autophagy* (2018)

Köln, den 23.04.2018

Alexander Gluschko

Curriculum vitae

Alexander Gluschko

geboren am 06.11.1984

in Kiewka (Kasachstan)

Familienstand: ledig

Staatsangehörigkeit: deutsch

Hochschulausbildung

2013 – 2018 Promotionsstudium am Institut für Medizinische Mikrobiologie, Immunologie und Hygiene, Universitätsklinikum Köln

Thema: “LC3-associated Phagocytosis induced by the β_2 integrin Mac-1 enhances Immunity to Infection with *Listeria monocytogenes*”

2010 – 2013 Masterstudium “Biomedical Sciences” an der Hochschule Bonn-Rhein-Sieg in 53359 Rheinbach

Abschluss: Master of Science

2006 – 2010 Bachelorstudium “Applied Biology” an der Hochschule Bonn-Rhein-Sieg in 53359 Rheinbach

Abschluss: Bachelor of Science

Zivildienst

2005 – 2006 Pflegeheim Haus Tusculum in 53809 Ruppichterorth

Schulbildung

1997 – 2005 Homburgisches Gymnasium Nümbrecht in 51588 Nümbrecht

Abschluss: Abitur